Translated from *Uspekhi Khimii* **59** 3–38 (1990) U.D.C. 541.138

The electrochemistry of short-lived intermediate species

V A Benderskii, A G Krivenko
Institute for Energy Problems of Chemical Physics, USSR Academy of Sciences, Moscow

ABSTRACT. The results of the study of the electrode reactions of hydrogen atoms, simple organic radicals, and ions with anomalous valence by pulse radiolysis and laser photoelectron emission from the metal into the solution have been reviewed.

The bibliography contains 119 references.

Contents

I.	Introduction	1
II.	Generation of short-lived intermediate species	2
III.	Kinetics of the change in the current of electrode reactions	2
IV.	Polarograms of the species generated by a variable photoelectron emission current	5
V.	Time-resolved polarograms of intermediate species	6
VI.	Electrode reactions of hydrogen atoms	7
VII.	Intermediate species of the electrochemical carbon cycle	10
VIII.	Electrochemistry of alkyl and hydroxylalkyl radicals	13
IX.	The pK scale for weak CH-acids	15
X.	Intermediate species of the electrochemical nitrogen cycle	16
XI.	Reduction of ions with anomalous valence	19
XII.	Summary	20

I. Introduction

Most electrochemical processes are many-electron processes consisting of a sequence of one-electron stages in which intermediate species (IS) are formed and undergo further transformations. Since these species usually have a higher free energy than the reagents and products, their formation determines the energy barrier of the process as a whole, characterised by the magnitude of the overvoltage. Thus the electrochemistry of IS is a necessary part of modern electrochemistry, just as the study of the chemical transformations of IS forms part of chemical kinetics in general. Since IS take part in electrode reactions and are present in the adsorbed state on the electrode or diffuse to it from the layer of the solution next to the electrode, in the electrochemistry of short-lived IS, methods making it possible to determine the concentration or the current of the electrode reactions of the IS immediately after their generation are used. Extensive use is made of non-stationary electrochemical methods in which the IS are generated by an initial current pulse, and their subsequent transformations are recorded from the changes in the current and the electrode potential. These methods have been used to study a large number of reactions of free radicals and ions with anomalous valence (see in particular the published review[1]) with characteristic transformation times greater than $10^{-3}-10^{-4}$ s. The study of more rapid processes involving IS is restricted by the electrical double layer charging currents with change in potential. This restriction has stimulated the development of the methods of pulse electrochemical radiolysis (PECR) and laser photoelectron emission from the metal into the electrolyte solution (LPE), in which the IS are generated at a constant electrode potential. The present review examines the principles of these new methods and summarises the main results of their application. Particular attention is paid to the LPE method, since PECR data have already been reviewed.[2,3]

The sequence of processes taking place in a solution after pulse photoelectron emission from a metal has now been studied in sufficient detail.[4,5] The emitted electrons, which usually have energies in the range 0.5–2 eV, are thermalised and hydrated in aqueous solution, and the hydrated electrons (e^-_{aq}) are situated at a distance $l \simeq 3$ nm from the electrode surface. These electrons either diffuse to the electrode and are returned to the metal or are captured by an acceptor added to the solution, forming IS in a layer with approximately the same dimensions next to the electrode. As a result of these rapid processes, which with nanosecond duration bring about the photo-emission of laser pulses, a source of IS is formed close to the electrode; these IS diffuse to the electrode and take part in electrode reactions, accompanied by a change in the current or potential. The kinetics of this change are determined directly by the rate constants of the electrode reactions, so that it is possible to measure their absolute values up to 10^8 s^{-1}. The absence in the LPE method of the diffusion restrictions characteristic of electrochemical measurements is due to the small size of the IS source, noted above. Another characteristic of the method is that the rate constants are measured at a small degree of coverage, independent of potential, of the surface by the IS, the quantity of which is controlled by the intensity of the laser pulses and usually does not exceed 10^{11} cm^{-2}. Despite the small magnitude of the emitted charge, the pulse currents in LPE are fairly high ($\gtrsim 10^{-1}$ A cm^{-2}), so that the influence of contaminants is less significant than in ordinary electrochemical measurements at low overvoltages.

While the rates of the generation of the IS are similar in the LPE and PECR methods, the first of these has two important advantages: the absence of interfering reactions of primary radiolysis products (primarily hydrogen peroxide) and diffusion restrictions. In PECR, as a result of the uniform generation of IS in the bulk of the solution, their currents are restricted by diffusion and bulk recombination, so that it is possible to measure the rate constants only in a comparatively narrow range from 10^3 s^{-1} to 10^5 s^{-1}. In the LPE method, as shown below, it is possible to measure constants in the range 10^0-10^7 s^{-1}.

The idea of using pulse photo-emission measurements to study the fast electrode reactions of IS was put forward as early as 1971,[6,7] but it was only several years later[8,9] that apparatus was developed for quantitative measurements.

II. Generation of short-lived intermediate species

By using radiation-chemical data[10,11] to select an acceptor, it is possible to obtain most IS of many-electron electrode processes, so that the PECR and LPE methods are universal. Table 1 gives the rate constants k_a of the reactions yielding the IS whose electrochemistry has been studied by LPE. When it is difficult to select an acceptor of e^-_{aq} to obtain a required species, as for example in the case of hydroxyalkyl radicals, use is made of the reactions of OH radicals and H atoms previously generated in the solution by the reaction of e^-_{aq} with nitrous oxide and hydrogen ions respectively. The reactions listed in Table 1 have been studied by pulse radiolysis with identification of the IS from the absorption spectra. Most IS have also been identified from the EPR spectra of irradiated frozen solutions of the corresponding acceptors.

Table 1. Rate constants for the reactions of IS formation, studied by LPE methods.[10]

a) Reactions involving e^-_{aq} acceptors

IS	Acceptor	$10^{-9}\,k_a$, $mol^{-1}\,s^{-1}$	IS	Acceptor	$10^{-9}\,k_a$, $mol^{-1}\,s^{-1}$
H	H_3O^+	8	$CFCl_2$	$CFCl_3$	16
OH	N_2O	6	CF_3	CF_3Cl	7
CH_3	CH_3Cl	1.1	CCl_3	CCl_4	30
C_2H_5	C_2H_5Cl	0.8	C_2H_4Cl	$C_2H_4Cl_2$	9
n-C_3H_7	**n-C_3H_7Cl**	0.7	HCO	H_2CO_2	0.2
n-C_4H_9	**n-C_4H_9Cl**	0.4	$(CH_3)_2COH$	$(CH_3)_2CO$	6
C_6H_5	C_6H_5Br	4	CO_2^-	CO_2	8
CH_2Cl	CH_2Cl_2	6	NO_3^{2-}	NO_3^-	11
$CHFCl$	$CHFCl_2$	3	NO_2^{2-}	NO_2^-	4
CHF_2	CHF_2Cl	3	NO^-	NO	30
$CHCl_2$	$CHCl_3$	30	NH_2	NH_2OH	0.9
CF_2Cl	CF_2Cl_2	14	BrO_2	BrO_3^-	3

b) Reactions involving OH acceptors

IS	Acceptor	$10^{-9}\,k_a$, $mol^{-1}\,s^{-1}$	IS	Acceptor	$10^{-9}\,k_a$, $mol^{-1}\,s^{-1}$
CH_2OH	CH_3OH	0.6	$CH_2CH(OH)Cl$	C_2H_3Cl	7
CH_2CH_2OH	C_2H_4	3	CO_2^-	HCO_2^-	3
CH_3CHOH	C_2H_5OH	2	NH_2O	NH_2OH	9

III. Kinetics of the change in the current of electrode reactions

The changes with time in the current or emitted charge in LPE are calculated by solving the non-stationary equations for the diffusion of e^-_{aq} and the IS. A detailed analysis has been published.[5,12,13] The concentration of e^-_{aq} is given by the equation

$$\partial n/\partial t = D_e\partial^2 n/\partial x^2 - k_a N_a n + \frac{I_0}{l}\exp(-x/l)\,f(t), \qquad (1)$$

where D_e is the diffusion coefficient of e^-_{aq}; k_a the rate constant of the capture of e^-_{aq} by the acceptor added to the solution to give a concentration N_a; I_0 the photo-emission current generated by the laser pulse, whose form is described by the time function $f(t)$; and l the characteristic dimension of the source of e^-_{aq}. Because of the high rate of the electrode reaction of e^-_{aq}, the quantity $n(0, t) = 0$. For the concentration of IS stable† in solution $n_1(x, t)$, the following equation is applicable:

$$\partial n_1/\partial t = D\partial^2 n_1/\partial x^2 + k_a N_a n. \qquad (2)$$

As a result of their diffusion, a flux of IS into the adsorption plane $x = 0$, equal to $\kappa_a n_1(0, t)$, is created, where κ_a is the rate constant of the adsorption, with dimensions cm s^{-1}. The adsorbed species are desorbed with a rate constant W_d and take part in the electrode reactions with an overall rate constant $W = W_2 + W_3$ (W_2 and W_3 are the rate constants of the oxidation and reduction of the IS respectively). The surface concentration of IS (Γ) obeys the equation

$$d\Gamma/dt = \kappa_a n_1(0, t) - (W_d + W)\Gamma. \qquad (3)$$

As a consequence of the continuity of the flux at $x = 0$ there arises the boundary condition

$$D(\partial n_1/\partial x)_{x=0} = \kappa_a n_1(0, t) - W_d\Gamma. \qquad (4)$$

This adsorption–desorption scheme for the electrochemically active IS is applicable if the degree of coverage is small, that is κ_a and W_d are independent of Γ. If the rate constant W is smaller than the rate of the processes involving e^-_{aq} and the reciprocal of the laser pulse duration t_0^{-1}, that is

$$W < D_e/l^2,\ k_a N_a,\ t_0^{-1}, \qquad (5)$$

the equation for the change in the current with time is independent of the duration of the laser pulse, the characteristic length of the source l, and the rate of capture of e^-_{aq}. From the solution of Eqns. (1) and (2) it follows[13] that the form of the kinetic curves of the charge emitted into the solution $Q(t)$ is determined by the parameter

$$\xi = 4\kappa_a W/W_d^2 D \qquad (6)$$

and, depending on its value, is described by one of the following relationships ($t > t_0$):

$$Q/Q_m = \begin{cases} 1 + \dfrac{W_3 - W_2}{W_3 + W_2}\,(1 - \exp(-Wt)), & \xi \gg 1; \\ 1 + \dfrac{W_3 - W_2}{W_3 + W_2}\left(1 - \dfrac{1}{\varkappa}\sqrt{\dfrac{D}{\pi t}}\right), & \xi \ll 1,\ \varkappa\sqrt{t/D} > 1, \end{cases} \qquad (7)$$

where Q_m is the number of e^-_{aq} captured by the acceptor, and κ the effective rate constant of the electrode reaction, determined by the quasi-stationary current

$$\varkappa = \kappa_a \frac{W}{W + W_d}. \qquad (8)$$

The rate constants for the adsorption and desorption are related by the detailed equilibrium condition

$$\frac{\kappa_a}{W_d} = \frac{\Gamma_0}{N_0}\exp\left(-\frac{\Delta G_a^0}{RT}\right), \qquad (9)$$

where ΔG_a^0 is the free energy of adsorption, corresponding to the selected standard bulk (N_0) and surface (Γ_0) concentrations. With allowance for Eqn. (9), the condition $\xi \gg 1$ means that the kinetic

† The case in which the IS is transformed in the bulk has been examined.[7] The stability of the IS means that the time of their homogeneous transformation is greater than the time of their movement to the electrode.

curves $Q(t)$ have an exponential form in the following range of values of W:

$$\frac{\varkappa_a^2}{D} > W > \frac{D}{4}\left(\frac{N_0}{\Gamma_0}\right)^2 \exp\left(\frac{2\Delta G_a^0}{RT}\right) = W_{\min}. \quad (10)$$

The upper boundary of the range is determined by the condition that W be small compared with the rate of adsorption. The opposite inequality corresponds to diffusion-controlled reactions, whose rate is limited by the transport of the reagent to the surface. The values of W in this case are greater than 10^8 s^{-1}, and cannot be measured by the LPE method, since the conditions (5) do not apply. The lower boundary depends on ΔG_a^0, and for $\Delta G_a^0 < -25$ kJ mol^{-1} does not exceed 1 s^{-1} for the following typical values of the other parameters: $N_0 = 64 \times 10^{20}$ cm^{-3} (standard 1 M solution), $\Gamma_0 = 10^{14}$ cm^{-2}, $D = 10^{-5}$ cm^2 s^{-1}, $T = 300$ K. Estimation of $W_{\min}$ shows that even for comparatively weakly adsorbed IS, the range of values of W satisfying relationship (10) is greater than $10^7 - 10^8$. When condition (10) is satisfied, there is no adsorption equilibrium, and the IS are not desorbed and take part in electrode reactions. Otherwise, when $\xi \ll 1$, adsorption equilibrium is established, the form of the kinetic curves changes, and $Q(t)$ is characterised by the effective rate constant κ, as in ordinary electrochemical measurements, under the conditions of a quasi-stationary current: $j_c = \kappa n_1(0)$. The range of values of κ that can be measured is restricted by the condition

$$\varkappa < \sqrt{W_{\min} D},\ \sqrt{k_a N_a D},\ \sqrt{D/t_0},\ D/l \quad (11)$$

from which it follows that the LPE method can be used to measure the rate constants of the electrode reactions of non-adsorbed IS ($\Delta G_a^0 \geqslant 0$) up to 30–50 cm s^{-1}.

It follows from conditions (7) that the kinetic curves $Q(t)$ are determined by the existence of two signals: the initial rapid signal corresponding to the photo-emission and return to the electrode of the e_{aq}^- not captured by the acceptor, and the subsequent slower signal due to the electrode reactions of the IS. The ratio of the amplitudes of these signals equal to $Q(t)/Q_m - 1$ as $t \to \infty$ corresponds to the number of electrons transferred from the metal to the solution, calculated for one electron captured by the acceptor, that is for one IS, so that $Q(\infty)/Q_m - 1$ is the order (n) of the electrode reaction

$$X + n e^- \rightarrow X^{n-} \quad (12)$$

with respect to electrons. The values of n, unlike W, can also be determined by measuring the relative values of the photo-current for stationary photo-emission into the solution being studied and into a solution for which n is known.[4,5] The latter are usually N_2O solutions, in which the capture of e_{aq}^- gives OH radicals, produced throughout the working range of the mercury electrode, so that $n = 1$.

$Q(t)$ is measured using the laser electrochemical relaxometer[5,9,14,15] (Fig. 1). The nitrogen laser with a wavelength of 337 nm, the fourth harmonic of the neodymium laser (265 nm), and excimer lasers (220 nm and 248 nm) [15] are used as light sources. To avoid the superposition of effects due to pulse heating to the electrode, the production of capillary waves (in the case of liquid metal electrodes), and decrease in the concentration of the acceptor in the layer next to the electrode, the light intensity is restricted to 700 kW cm^{-2} for a pulse duration of $\sim 10^{-8}$ s. The range 20–200 kW cm^{-2} is most convenient for the measurements. The restriction of the light intensity and the low quantum yield of the photo-emission ($\sim 10^{-4}$ A W^{-1}) make it necessary to record the weak signals in a broad frequency band. It is most convenient to use a stroboscopic recording scheme, employing laser pulses with a repetition frequency of 6–25 Hz and a signal measured at a given moment of time (relative to the laser pulse) and a given electrode potential. The signal recording time is 30–40 s, so that it is possible to average over a large number ($\sim 10^3$) of pulses. With time scanning, the relaxometer can be used to obtain the kinetic curves $Q(t)$, and when the potential E is scanned, it gives the $Q(E)$ relationship at the selected moment of time. A design feature of the cell with the mercury electrode, ensuring suppression of capillary waves, is the use of a photocathode with a flat mercury surface which is kept in an amalgamated platinum capillary and is replaced after each scanning cycle.

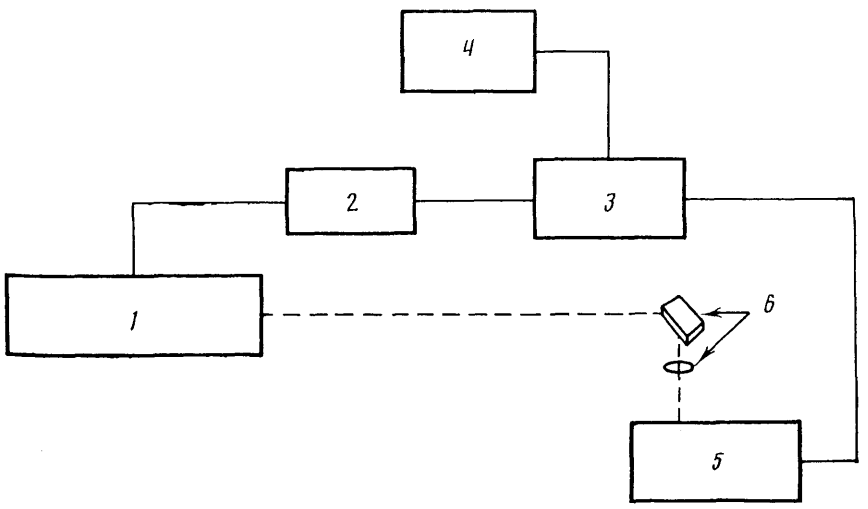


Figure 1. Block diagram of the laser electrochemical relaxometer: *1*, photon generator; *2*, synchronisation system; *3*, stroboscopic oscillograph; *4*, recorder; *5*, measuring cell with amplifier and polarisation scheme; *6*, laser beam focussing system.

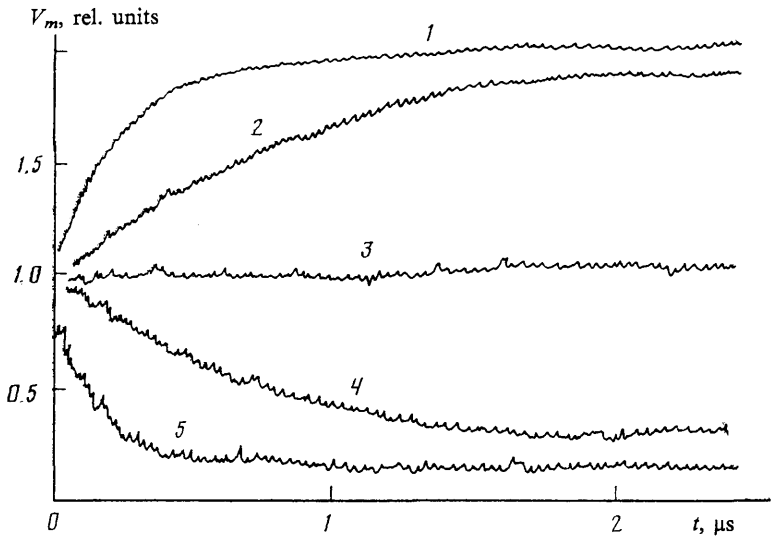


Figure 2. Kinetic curves for the electrochemical reduction and oxidation of H atoms in 1 M aqueous KCl solution with the addition of 0.1 M HCl at different values of the potential of the mercury electrode, V: *1*, −0.9; *2*, −0.7; *3*, −0.55; *4*, −0.5; *5*, −0.4.

The recorded signal $V(t)$ is equal to the variation in the electrode potential brought about by the change in its charge, and is given by the relationship[5]

$$V(t) = \frac{1}{C}\int_0^t \frac{dQ(t')}{dt'} \exp\left(-\frac{t-t'}{\tau_0}\right) dt', \qquad (13)$$

where C is the capacity of the electrical double layer; $\tau_0 = RC$ the time constant of the electrochemical cell and the input circuit; and R their total ohmic resistance. From Eqns. (7) (for $\xi \gg 1$) and (13) it follows that

$$\frac{V}{V_m} = \frac{2W_3\tau_0 - 1}{W\tau_0 - 1} \exp(-t/\tau_0) - \frac{(W_3 - W_2)\tau_0}{W\tau_0 - 1} \exp(-Wt), \; t \gg t_0, \qquad (14)$$

where $V_m = Q_m/C$. For $W\tau_0 \gg 1$, $V(t) = Q(t)/C$. These charge measurement conditions are used for values of W from 10^7 s^{-1} to 10^4 s^{-1}, since τ_0 is usually equal to $10^{-3}-10^{-4}$ s. The rate constants of slower reactions are measured using current conditions in which $W\tau_0 \ll 1$ and

$$V/V_m = \exp(t/\tau_0) + (W_3 - W_2)\tau_0 \exp(-Wt). \qquad (15)$$

To extend the range of measurement of the constants under current conditions, τ_0 is decreased, and t_0 is increased. The use of current–voltage transformers with an input resistance close to zero decreases to τ_0 to 3–5 μs, so that the highest values of W that can be measured under current conditions are 10^5 s^{-1}.[16] $W \leqslant 10^3$ s^{-1} are measured using the pulses of a continuous helium–cadmium laser (λ = 325 nm) produced by a mechanical modulator; periodic illumination methods are also used.[17] The combination of the two measurement conditions (charge and current) makes it possible to cover the range of values of W from 1 s^{-1} to 10^7 s^{-1}, satisfying the inequalities (10).

The kinetic curves are treated using relationships (14) and (15). The accuracy of the determination of W is restricted by the scatter in the amplitude of the laser pulses, and is generally 10–15%. Eqns. (7) show that the form of the kinetic curves deviates from the exponential for $\xi \simeq 1$. For electrode reactions whose characteristic time is less than 10^{-4} s, $\xi \leqslant 1$ at rates of desorption greater than 10^5 s^{-1}, that is in the case where there is practically no adsorption of the species ($\Delta G_a^0 > -10$ kJ mol^{-1}). Analysis of the $V(t)$ curves makes it possible not only to determine the absolute values of W or κ but also to establish the state (adsorbed or not) in which electron transfer takes place.

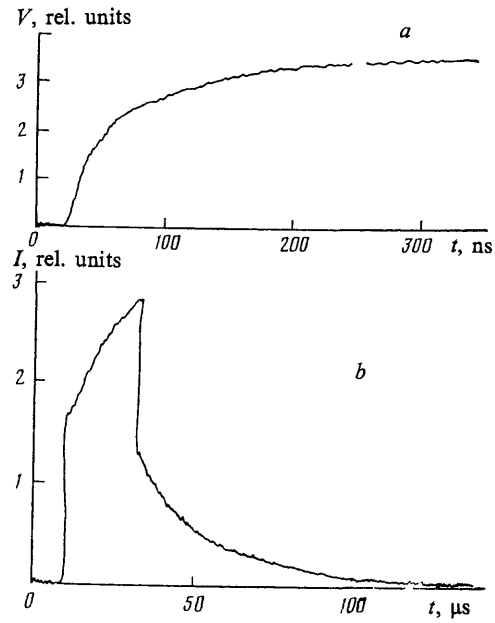


Figure 3. Form of the kinetic curves for the reduction of the Ch_2Cl radical adsorbed on a mercury electrode: *a*, under charge measurement conditions (E = −1.67 V, $W_3 = 1.4 \times 10^7$ s^{-1}), *b*, under current measurement conditions (E = −0.89 V, W_3 = 30 s^{-1}, laser pulse duration 20 ms).[16]

Typical $V(t)$ curves are given in Figs. 2 and 3. The changes in the form and characteristic times of these curves are due to the

changes in W_2 and W_3 with change in the electrode potential.‡ The rate of the rapid reactions of adsorbed hydrogen atoms are measured under charge conditions. In the cathodic potential range, in which the reduction of H atoms predominates, the $V(t)$ curves consist of a short initial section and a section corresponding to the slower doubling of the emitted (captured by the acceptor) charge ($W_3 \gg W_2$, $n = 1$). The characteristic rise time, that is W_3^{-1}, decreases with increase in $-E$. For anodic displacement of E, the rise time increases, and the amplitude in the "slow" section decreases. At the characteristic potential E^*, when the rate constants of the reduction and oxidation become equal:

$$W_2(E^*) = W_3(E^*) = W^*, \tag{16}$$

the "slow" section disappears, since when oxidation and reduction are equally probable (and when the values of n are identical), the transformations of the IS do not change the charge of the electrode. For $E > E^*$, the magnitude of $V(t)$ decreases from the initial value V_m to $V_m W_3/(W_2 + W_3)$, since the main channel for the transformation becomes the ionisation of H atoms, leading to the return to the electrode of the emitted electrons and the electrons captured by the acceptor ($n = -1$). The decay time of $V(t)$ decreases with increase in E as a result of the increase in W_2. Fig. 3 gives the $V(t)$ curves corresponding to the reduction of the CH_2Cl radical, for which the $W_3(E)$ relationship can be measured over a range of change in $W_3(E)$ of almost 10^7.

IV. Polarograms of the species generated by a variable photoelectron emission current

Varying illumination with a frequency of Ω creates an IS flux in phase with it, with a characteristic source length $l_1 \simeq \sqrt{D/k_a N_a} \simeq 10^{-5}-10^{-6}$ cm, so that at the low frequencies usually employed $l_1 \ll \sqrt{D/\Omega}$ and the resulting photo-emission current, as in the case where the inequalities (5) are satisfied, is independent of the conditions under which the IS are formed. Without forgetting that photoemission gives IS and not stable reagents, the obvious similarity in the methods used to observe the polarograms and the photocurrent should be emphasised. In polarography, a stationary flux of the reagent to the electrode is maintained by its constant concentration at the outer boundary of the Nernst layer (see for example the works by Bond[1] and Damaskin and Petrii[18]), and in the version of the LPE method being considered it is maintained by the constant amplitude of the current of the emitted electrons, which, like the diffusion polarographic current, determines the height of the polarographic wave. Although the reasons for the production of the limiting current are different in the two cases being considered, the polarisation dependence of the photocurrent coincides with the polarographic wave. The range of Ω suitable for observing the polarograms of IS is restricted by the conditions of small interfering charging currents and convective mixing of the layer with a thickness $\sqrt{D/\Omega}$:

$$\tau_0^{-1} > \Omega > D/\delta^2, \tag{17}$$

where $\delta \simeq 10^{-2}$ cm is the thickness of the Nernst layer in the absence of forced mixing. The range of electrode reaction rate constants ($\kappa \simeq \sqrt{D\Omega}$) that can be measured in this range of Ω ($0.1-3 \times 10^3$ Hz) is $10^{-3}-1$ cm s^{-1}.

The form of the polarographic waves for a periodic photoemission current has been analysed.[17,19–22] The solution of Eqns. (1) and (2) under the conditions in which a periodic source is used shows that the amplitude and phase of the first harmonic of the photocurrent in the irreversible n-electron reduction of a non-adsorbed product of the capture of e_{aq}^- are given by the relationship

$$j = \frac{I}{I_0} = \left| 1 + n\frac{v_1}{v_1 + \sqrt{2i}} \right|, \quad \operatorname{tg}\Phi = -\frac{nv_1}{((1+n)v_1 + 1)(v_1+1)+1}, \tag{18}$$

where I is the measured photocurrent, I_0 the current for the formation of the IS, equal to the difference between the currents of the photoemission and the return to the electrode of the e_{aq}^- not captured by the acceptor, and $v_1 = \kappa_1\sqrt{2/D\Omega}$. When the rate constant of the reduction κ_1 obeys the equation of retarded discharge

$$\kappa_1 = \kappa_{10}\exp(\alpha\eta), \quad \eta = \frac{e}{kT}(E^0 - E), \tag{19}$$

(E^0 is the standard potential, and α the transfer coefficient), the $j(E)$ relationship has the form of a polarographic wave in which j increases from 1 to $1 + n$. The half-wave potential of the one-electron reduction, for which $j = 3/2$, is

$$E_{1/2} = E^0 - \frac{1}{2\alpha}\ln\left(0.91\,\frac{D\Omega}{\kappa_{10}^2}\right). \tag{20}$$

With increase in Ω, the potential $E_{1/2}$ increases in logarithmic proportion while the form of the wave is preserved. The slope of the wave in the region of $E_{1/2}$, equal to $(dj/dE)_{E=E_{1/2}}$, is independent of Ω and equal to $0.29\alpha kT/e$. The wave for the irreversible reduction of adsorbed IS is described by the relationships

$$j = \left| 1 + n\frac{W_3}{W_3 + i\Omega} \right|, \quad \operatorname{tg}\Phi = -\frac{n\Omega W_3}{(1+n)W_3^2 + \Omega^2} \tag{21}$$

and its slope in this case is approximately twice that for non-adsorbed species. The phase shift is greatest close to $E_{1/2}$, and is several times greater for adsorbed species than for non-adsorbed species. The wave for the reversible reduction of non-adsorbed IS ($X + ne^- \leftrightharpoons X^{n-}$) is described by the equation

$$j = \left| 1 + n\frac{v_1}{v_1 + v_2 + \sqrt{2i}} \right|. \tag{22}$$

Here, $v_2 = k_2\sqrt{2/D\Omega}$, where κ_2 is the rate constant of the back reaction of X^{n-} oxidation. The potential of the reversible half-wave is equal to the standard redox potential X^{n-}/X, and its slope is $nkT/4e$, like the slope of the usual reversible polarographic wave under stationary diffusion conditions.[18] The wave remains reversible, and $E_{1/2} = E^0$, when $\Omega \ll 2\kappa_{10}^2/D$. At higher values of Ω, the wave becomes irreversible, it is displaced along the E axis, its slope decreases, and a phase shift is produced. The characteristics of the E-waves for the one-electron reduction and oxidation of IS are summarised in Table 2.

The wave for the n-electron irreversible reduction with previous irreversible transformation of the primary IS ($X \rightarrow Y \rightarrow Y^{n-}$) is described by the relationship

$$j = \left| 1 + n\frac{v_1}{v_1 + \sqrt{2i}}\,\frac{\sqrt{\beta_1 + 2i} - \sqrt{2i}}{\sqrt{\beta_1 + 2i}} \right|. \tag{23}$$

Here, $\beta_1 = 2k_1/\Omega$, where k_1 is the rate constant of the homogeneous

‡ All the values of E except the standard values are given relative to the saturated calomel electrode.

reaction X → Y. As in the case of ordinary polarographic *CE*-waves, a limiting current determined by the rate of the chemical stage is produced. With increase in Ω, the height of the wave (the amplitude of the limiting current) decreases, and the wave is displaced to more negative potentials. When the chemical stage is reversible and the rate constant of the back reaction k_2 is appreciably greater than the rate constant of the homogeneous reaction k_1, the limiting current j_∞ is determined by the equilibrium constant of this stage:

$$j_\infty = \left| 1 + n \frac{p}{p + \sqrt{2i}} \right|, \text{ where } p = \frac{k_1}{k_2} \sqrt{\frac{k_1 + k_2}{\Omega}}. \quad (24)$$

As an example of a *CE*-wave, Fig. 4 gives the $j(E)$ relationships for the three-electron reduction of NO to NH_2OH. The reversible chemical stage preceding the electrode reaction is the protonation of NO in the presence ot NH_4^+ ions.[23]

Table 2. Characteristics of the *E*-waves of the one-electron reduction (oxidation) of the intermediate species generated by a periodic photoelectron emission current.[22]

Mechanism of reduction (oxidation)	Relationships		
	$\eta_{1/2}$ (Ω)	$(dj/d\eta)_{\eta=\eta_{1/2}}$	$\operatorname{tg} \varphi_m^*$
$A \underset{(\varkappa_2)}{\overset{\varkappa_1}{\rightarrow}} B$	$a \ln\left(bD\Omega/\varkappa_0^2\right)$, where $a = \frac{1}{2}\alpha(\frac{1}{2}\beta)$, $b = 0.91$ (1.35)	0.291 α (0.282 β)	−0.143 (0.451)
$A_{ads} \underset{(W_3)}{\overset{W_3}{\rightarrow}} B$	$a \ln(b\Omega/W_0)$, where $a = 1/\alpha$ (1/β), $b = 0.84$ (1.73)	0.486 α (0.375 β)	−0.354 (1.73)
$A \underset{\varkappa_2(\varkappa_1)}{\overset{\varkappa_1(\varkappa_2)}{\rightleftarrows}} B$	0 (0)	0.25 (0.25)	$-0.17\sqrt{D\Omega/\varkappa_0^2}$ $\left(0.35\sqrt{D\Omega/\varkappa_0^2}\right)$
$A_{ads} \underset{W_2(W_3)}{\overset{W_3(W_2)}{\rightleftarrows}} B_{ads}$	0 (0)	0.25 (0.25)	$-0.17\,\Omega/W_0$ $(0.5\,\Omega/W_0)$
$A_{ads} \underset{\varkappa_2(\varkappa_1)}{\overset{W_3(W_2)}{\rightleftarrows}} B$	$a \ln\left(b\varkappa_0^2\Omega/W_0^2 D\right)$, where $a = \frac{1}{2}(-\frac{1}{2})$, $b = 0.91$ (1.35)	0.291 (0.272)	−0.143 (0.451)
$A \underset{W_2(W_3)}{\overset{\varkappa_1(\varkappa_2)}{\rightleftarrows}} B_{ads}$	$a \ln\left(b\varkappa_0^2\Omega/W_0^2 D\right)$, where $a = -\frac{1}{2}(\frac{1}{2})$, $b = 1.10$ (0.91)	0.291 (0.272)	0.143 (0.451)

* In oxidation reactions the phase shift reaches π/2. Here the values of tan φ for $E = E_{1/2}$ are given.

Since most IS are capable of undergoing both reduction and oxidation, the $j(E)$ relationships usually have the form of cathodic–anodic waves. For one-electron irreversible processes ($n = \pm 1$) involving non-adsorbed and adsorbed IS, their form is determined by the relationships:

$$j = \left| 1 + \frac{v_1 - v_2}{v_1 + v_2 + \sqrt{2i}} \right|, \quad \operatorname{tg} \Phi = -\frac{v_1 - v_2}{(2v_1 + 1)(v_1 + v_2 + 1) + 1}$$

or

$$j = \left| 1 + \frac{W_3 - W_2}{W_2 + W_3 + i\Omega} \right|, \quad \operatorname{tg} \Phi = -\frac{(W_3 - W_2)\,\Omega}{2W_3(W_2 + W_3) + \Omega^2} \quad (25)$$

The potential at which $j = 1$ is equal to E^*. The slope of the cathodic–anodic wave at $E = E^*$ is determined by the sum of the transfer coefficients

$$\left(\frac{dj}{dE}\right)_{E=E^*} = \frac{v^*(1 + 2v^*)}{(1 + 2v^*)^2 + 1}(\alpha + \beta)\frac{kT}{e} \text{ or}$$
$$\left(\frac{dj}{dE}\right)_{E=E^*} = \frac{2W^{*2}}{\Omega^2 + 4W^{*2}}(\alpha + \beta)\frac{kT}{e}. \quad (26)$$

Here, $v^* = \varkappa^*\sqrt{2/D\Omega}$, where $\varkappa^*$ is the value of the constants for $E = E^*$, when the rates of oxidation and reduction are equal. According to Eqns. (26), as $\Omega \to 0$ the slope of the cathodic–anodic wave is equal to $(\alpha + \beta)kT/2e$ and decreases with increase in Ω. The wave is then split into separate cathodic and anodic components, and the difference in the half-wave potentials increases logarithmically. Splitting of the cathodic–anodic wave with increase in Ω has been observed for alkyl and hydroxyalkyl radicals.[24] The determination of the rate constants and transfer coefficients becomes possible in the split wave.

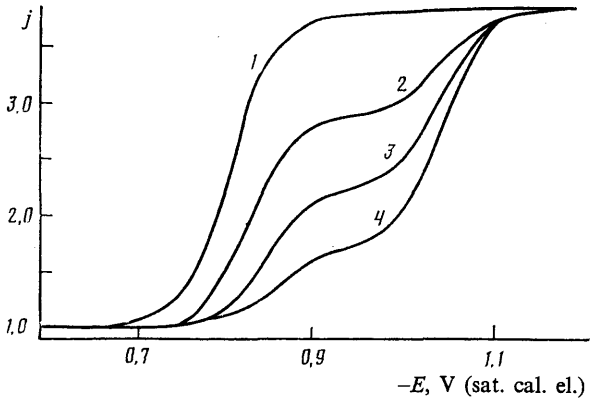


Figure 4. Polarograms for the three-electron reduction of NO, generated by a photoelectron emission current with a frequency of 1, 6.4, 29, and 87 Hz (curves *1*–*4* respectively) in aqueous 0.5 M Na_2SO_4 + 0.5 M $(NH_4)_2SO_4$ + 10^{-3} M $NaNO_2$.[23]

The analysis of the form and phase of the polarograms over a wide frequency range makes it possible to study fairly complex IS transformations.[22]

V- Time-resolved polarograms of intermediate species

The $Q(E)$ relationship at a fixed moment of time t for the one-electron reduction and oxidation of adsorbed IS has the form:[25]

$$q(\varphi, \tau) = \frac{Q(\varphi, \tau)}{Q_m} = 1 + (1 - \exp(-\tau(e^{\alpha\varphi} + e^{-\beta\varphi})))\operatorname{th}\frac{\alpha + \beta}{2}\varphi, \quad (27)$$

where

$$\varphi = \frac{e}{kT}(E^* - E), \quad \tau = W^* t,$$

and the rate constants of the oxidation and reduction are described by the equations for retarded discharge

$$W_2 = W^* \exp(-\beta\varphi), \quad W_3 = W^* \exp(\alpha\varphi). \tag{28}$$

Eqn. (27) describes a time-resolved cathodic–anodic wave. The quantity $q(\tau)$ is the number of electrons transferred to the solution, calculated for one IS at the moment of time t after its formation. If the species is not adsorbed, the $q(\varphi, \tau)$ relationship is described by the expression

$$q(\varphi, \tau) = 1 + (1 - w(a_1(e^{\alpha\varphi} + e^{-\beta\varphi}))) \operatorname{th} \frac{\alpha+\beta}{2}\varphi, \tag{29}$$

where

$$w(z) = e^{z^2} \operatorname{erfc} z, \quad a_1 = \varkappa_a \frac{W^*}{W^* + W_d} \sqrt{\frac{t}{D}}. \tag{30}$$

It follows from Eqns. (27) and (29) that the splitting of the cathodic–anodic wave takes place in a narrow range $t^{-1} \sim W^*$. For $W^*t < 1$, two waves are observed with a section $q = 1$ close to E^*, which becomes narrower with increase in t. When $W^*t > 1$, one wave is produced

$$q_{in}(\varphi) = 1 + \operatorname{tn}\left(\frac{\alpha+\beta}{2}\varphi\right).$$

Fig. 5 gives the time-resolved polarograms for the CH_2OH radical. The asymmetry of the cathodic and anodic waves is due to the difference in the transfer coefficients for W_2 and W_3. If the electrode reactions are accompanied by the destruction of IS not associated with electron transfer, then the section $q = 1$ does not disappear even when $W^*t > 1$. This has been observed for CH_3 radicals,[24] whose recombination is more rapid than the electrode reactions in the region of E^*. As an example of the time-allowed polarogram of a many-electron reduction, Fig. 6 gives the $q(\varphi, \tau)$ relationships for the BrO_2 radical.[25] For $t = 0.25$ μs and 0.5 μs and $E \geqslant -0.9$ V, the radical is unable to undergo complete reduction to BrO_2^-, which is formed quantitatively at $E < -0.9$ V ($n = 1$). The bromite ion is reduced at $E < -1.15$ V. The extent of the reduction increases with increase in t and $-E$. At $t > 50$ μs, the waves for the reduction of BrO_2 and BrO_2^- are not resolved, and the overall five-electron wave for the formation of Br^- is observed.

The time-resolved polarograms obtained under charge measurement conditions can be used to study more rapid processes than when a periodic photoemission current is used.

Examples of polarograms obtained by the PECR method have been published.[2,3,26] Unlike the polarograms obtained by the LPE method, they show a broad range of E values in which $j = 0$, due to the more rapid recombination of the IS, compared with the electrode reactions.

VI. Electrode reactions of hydrogen atoms

The adsorbed hydrogen atom is an IS in the electrochemical liberation of hydrogen (ELH), which in the case of metals with a high overvoltage includes a stage involving the discharge of hydrogen ions

$$H^+(aq) + e^- \xrightarrow{\varkappa_1} H_{ads}, \tag{31}$$

the reverse ionisation stage

$$H_{ads} \xrightarrow{W_2} H^+(aq) + e^- \tag{32}$$

and electrochemical desorption, in which the proton donors (PD) are water molecules and hydrogen ions[18,27–29]

$$H_{ads} + H_2O + e^- \xrightarrow{W_{30}} H_2 + OH^- \tag{33}$$

$$H_{ads} + H^+(aq) + e^- \xrightarrow{W_{31}} H_2. \tag{34}$$

The detailed study of the polarisation relationships observed when low-frequency photocurrents ($W \gg \Omega$) are used in solutions of acids[4,5,30–33] has established that the value of E^* depends on the pH of the solution, since a linear relationship exists between the overall rate constant of the electrochemical desorption and the concentration of hydrogen ions (N_{H^+}):

$$W_3 = W_{30} + W_{31}N_{H^+}. \tag{35}$$

The sum of the transfer coefficients of reactions (32) and (34) at a mercury electrode was found to be close to 0.5. Since the transfer coefficient for the discharge of hydrogen ions (α_1) at high overvoltages is equal to 0.5 and is related to β by the detailed balance condition ($\alpha_1 + \beta = 1$), it follows from the photo-emission data that the value of α in electrochemical desorption reactions is small, that is these exothermic reactions are almost activationless.

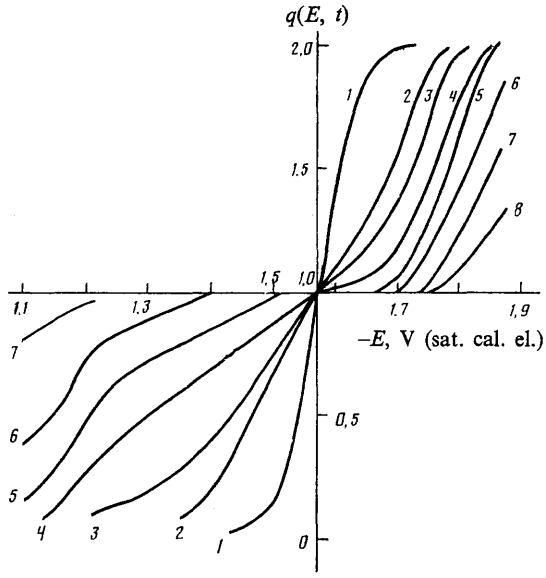


Figure 5. Time-resolved polarograms of the hydroxymethylradical adsorbed on a mercury electrode; photo-emission in 0.5 M KCl + 0.2 M CH_3OH + 2×10^{-2} M N_2O;[25] the curves correspond to the following instants of time, s: *1*, stationary; *2*, 10^{-4}; *3*, 5×10^{-5}; *4*, 2×10^{-5}; *5*, 10^{-5}; *6*, 5×10^{-6}; *7*, 2×10^{-6}; *8*, 10^{-6}.

The first measurements of the absolute values of the rate constants of electrochemical desorption[8] showed that W_3 is about 10^6 s^{-1}. Quantitative measurements have been carried out.[31,34–36] The kinetic curves $Q(t)$ are exponential, that is the hydrogen atoms take part in the electrode reactions after adsorption. The overall rate constant is described by Eqn. (35). The values of W_{30} and W_{31} are given in Table 3. It has been found[33,34] that the rate constant of reaction (34) on mercury and bismuth shows an exponential

dependence on the electrode potential, but is independent of temperature (Fig. 7). This relationship, which differs from that expected from the theory of retarded discharge, has been attributed[29,34,35] to the tunnel transfer of an electron from the metal to the reaction complex $H_{ads}-H_3O^+$. Since the change in the height of the barrier for electron tunnelling is equal to the change in the electrode potential, the rate constant of the tunnel electrode reaction shows an exponential dependence on E, but is independent of T. The electron transfer is accompanied by a simultaneous quantum displacement of the proton along the reaction coordinate, and this is the reason for the observed isotopic H/D effect. The model[34,35] predicts a decrease in W_{31} and an increase in the isotope effect with increase in both the energy of the M–H bond and the energy of reorganisation along the coordinate of the proton. The increase in the isotope effect on going from Hg to Bi and Ga (Table 3), when the energy of the bond between the H atom and the metal surface increases by 30–34 kJ mol,[37] is apparently due to the first of these factors, and the fact that the isotope effect is greater for Ga than for Bi indicates that reaction (34) involves a greater quantum displacement of the proton on the gallium electrode. This suggestion agrees with the high values of the isotope separation factors for hydrogen and tritium, characteristic of ELH reactions on Ga.[28] The measured values of W_{31} correspond to an electron tunnelling length of 4–5 Å for a height of the parabolic barrier of about 1.5 eV. The $W_{31}(E)$ relationship is described by the expression

$$W_{31}(E) = W_{31}(E^0)\exp\left(\frac{e(E^0-E)}{\gamma}\right), \qquad (36)$$

in which the value of γ is related to the tunnelling parameters of the electron and the proton. The values of γ for Hg, Bi, and Ga are 0.12, 0.18, and 0.17 eV respectively.

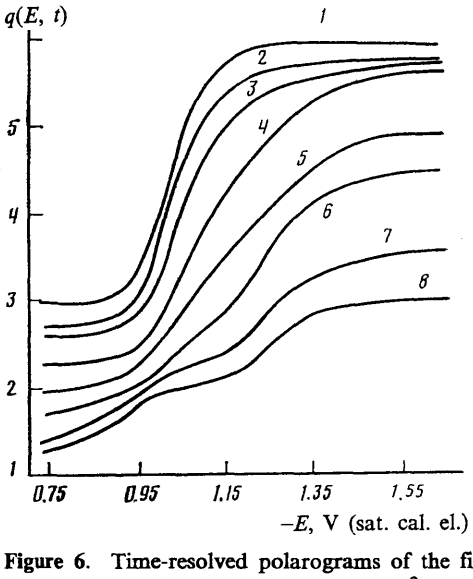


Figure 6. Time-resolved polarograms of the five-electron reduction of the BrO_2 radical in 0.5 M KCl + 10^{-2} M $KBrO_3$ solution;[25] the curves correspond to the following instants of time, s: *1*, stationary; *2*, 10^{-4}; *3*, 5×10^{-5}; *4*, 10^{-5}; *5*, 3×10^{6}; *6*, 10^{-6}; *7*, 0.25×10^{-6}.

The rate constant of reaction (33) depends little on E (Table 3), and its temperature dependence is characterised by an activation energy of ~15 kJ mol^{-1}, which remains unchanged in the electrode potential. The mechanism of this reaction has not been satisfactorily explained. From the value given for the activation energy, typical of dipole relaxation in water, and the times of this relaxation in the double layer ($10^{-8}-10^{-7}$ s),[38] it has been suggested[36] that the rate of reaction (33) is limited by the rate of the orientational rearrangement of the water molecules in the reaction complex. The values of W_{30} correspond to the bimolecular rate constants of reaction (33), which are ~10^{-3} times smaller than those for reaction (34).

Table 3. Rate constants of the electrochemical desorption of hydrogen and deuterium.[35,36]

Constant	Electrode	Value* of the constant at −E, V					
		0.9	1.0	1.1	1.2	1.3	1.4
$10^{-6}W_{30}$, s^{-1}	Ga **	—	1.9	2.1	2.8	3.6	4.3
			1.0	1.0	1.6	1.8	2.1
	Hg	1.0	1.6	3.1	5.7	9.0	—
		0.9	1.5	3.0	4.0	7.8	—
	Bi	—	0.03	0.09	0.13	0.16	0.18
			0.02	0.05	0.05	0.08	0.09
$10^{-8}W_{31}$, mol^{-1} s^{-1}	Ga **	—	0.4	1.3	1.9	3.3	5.2
			0.1	0.25	0.45	0.9	2.0
	Hg	0.30	0.75	1.4	3.4	8.0	—
		0.16	0.48	0.9	2.0	5.5	
	Bi	—	0.06	0.11	0.16	0.30	0.54
			0.03	0.05	0.07	0.15	0.27

* The upper row refers to H atoms, and the lower row to D atoms [$D^+(aq)$ ions in D_2O].
** Liquid electrode at 38 °C.

Ammonium ions are stronger PD than water molecules. The rate constants of electrochemical desorption involving them

$$H_{ads} + NH_4^+ + e^- \rightarrow H_2 + NH_3 \qquad (37)$$

on mercury are ~50 times greater than those for reaction (33) for identical values of $\gamma \simeq 0.18$ eV.

The ratio W_{31}/W_{30} increases with increase in $-E$ (Table 3), so that at low overvoltages, reaction (33) becomes the main reaction.

The electron transfer coefficient in electrochemical desorption from a polycrystalline gold electrode at $E \geqslant -0.1$ V increases to ~0.5,[32] that is there is a change from the activationless reaction to the normal reaction described by Eqn. (19), in accordance with the general ideas of the theory of electrode reactions.[28]

By comparing the values of W_3 measured by the LPE method with the ELH current

$$j_0 = 2ex_1N_{H^+}W_3/(W_2+W_3), \qquad (38)$$

it is possible to find the surface concentration of H_{ads}:

$$\Gamma_H = j_0/2eW_3. \qquad (39)$$

Eqn. (39) follows directly from the quasi-stationary character of the ELH current, and is not based on any model considerations. The calculated $\Gamma_H(E)$ relationships are given in Fig. 8. The values

of Γ_H depend little on N_{H^+}, since W_3, like j_0, is proportional to N_{H^+}, when $W_{31}N_{H^+} > W_{30}$. The increase in Γ_H on going from Hg to Ga and Bi is due to the increase in κ_1, and the fact that the values of Γ_H are higher on Bi than on Ga is due to the decrease in W_3. The value of Γ_H does not exceed 3×10^{12} cm^{-2} on all three metals, and is small for measurements by the usual electrochemical methods.

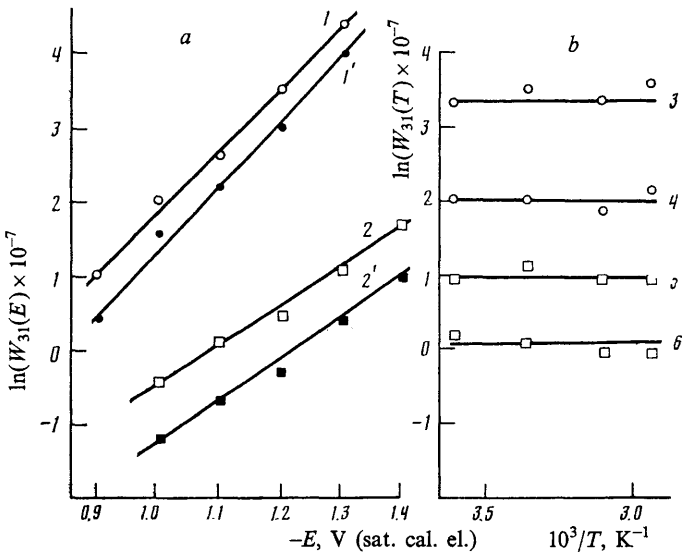


Figure 7. Dependence of the rate constant of the electrochemical desorption of hydrogen according to reaction (34) on the electrode potential (*a*) in H_2O (straight lines *1* and *2*) and D_2O (*1'*, *2'*) and on temperature (*b*) (straight lines *3*—*6*) on mercury (*1*, *1'*, *3*, *4*) and bismuth (*2*, *2'*, *5*, *6*) electrodes; the $W_{31}(E)$ relationships were measured at 22 °C, and $W_{31}(T)$ at $-E$ = 1.2, 1.0, 1.3, and 1.1 V (straight lines *3*—*6* respectively).[34]

The rate constants for the ionisation of H_{ads} on Hg were first measured by Benderskii and co-workers.[39,40] The $W_2(E)$ relationship is given in Fig. 9. In the range of E values from −0.6 V to −0.2 V, W_2 increases from 10^5 s^{-1} to 2×10^7 s^{-1} (β = 0.4—0.5), and in the range from −0.2 V to −0.1 V the transfer coefficient β decreases to 0.05—0.1. The decrease in β means that close to the equilibrium potential of ELH, the transfer coefficient for the direct reaction of hydrogen ion discharge (31) increases, tending to $\alpha_1 \simeq 1.0$, that is the Tafel law ($\alpha_1 = 0.50 \pm 0.05$), applicable for ELF at high overvoltages,[29,41] breaks down, and reaction (31) becomes barrierless. The suggestion that there is no barrier to the discharge of hydrogen ions at low overvoltages was previously put forward[42] (see also the book by Krishtalik[28]) on the basis of the fact that the overvoltage is independent of the composition of concentrated solutions of the anions adsorbed, although the data obtained,[42] like those in subsequent studies,[30,31] did not exclude a change not to barrier-free discharge but to quasi-equilibrium ($W_2 \gg W_3$) discharge, when it follows from Eqn. (38) that the effective transfer coefficient also becomes equal to 1. The results obtained by Babenko and co-workers[40] provide direct experimental confirmation of the existence of the barrier-free electrode processes assumed by Krishtalik.[42]

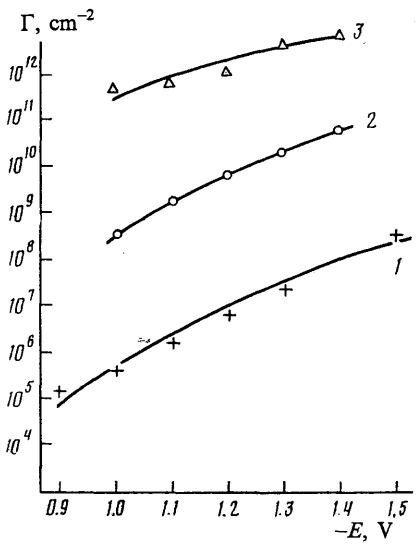


Figure 8. Surface concentration of hydrogen atoms adsorbed on mercury (*1*), liquid gallium (*2*), and bismuth (*3*).[36]

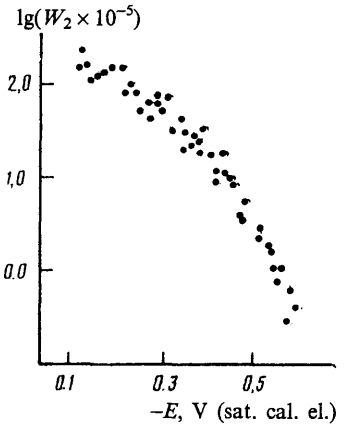


Figure 9. Dependene of the rate constant of the ionisation of hydrogen, adsorbed on mercury, on the electrode potential (0.3 M aqueous NaF solution with the addition of 0.01—0.03 M HF).[40]

As a result of the change in the transfer coefficients, the ELH exchange current on mercury is ~150 times smaller than that calculated by extrapolating the Tafel law to zero overvoltage (3×10^{-15} A cm^{-2} instead of 4×10^{-13} A cm^{-2}). A decrease in β analogous to that observed[40] for the mercury electrode was also observed on Au.[32] According to the detailed equilibrium principle,

the rate constants of reactions (31) and (32) are related by the thermodynamic expression

$$\frac{\kappa_1(E)}{W_2(E)} = \frac{\Gamma_H^0}{N_{H^+}^0} \exp\left(\frac{\Delta G(E)}{RT}\right), \quad (40)$$

where ΔG is the free energy of the discharge of $H^+(aq)$, and the values of Γ_H^0 and $N_{H^+}^0$ relate to the standard states. Eqn. (40) and the measured values of W_2 and j_0 can be used to find ΔG. When $\Gamma_H^0 = 10^{15}$ cm^{-2} (degree of coverage 1/2) is taken as standard state, the standard free energy ΔG^0 is 99.4 ± 3 kJ mol^{-1} (1.03 ± 0.03 eV). This agrees with the value found[42] from the temperature dependence of the barrier-free discharge current. The free energy of the adsorption of H atoms on mercury, equal to $\Delta G_H^0 - \Delta G$, is −104.1 ± 3 kJ mol^{-1}. The entropy of H_{ads}, according to an estimate[39] from the frequencies of the vibrations of the H atoms on the surface, does not exceed 8 J mol^{-1} K^{-1}, so that the energy of the Hg−H bond in the adsorbed state ($E_H = -\Delta G_a - T\Delta S_a$) is 136 ± 6 kJ mol^{-1}, confirming Frumkin's estimate of this quantity.[43]

Table 4. Values of E^0 and E^* for the two-electron stages of the electrochemical carbon cycle.[50]

Stage	pH	E^0, V (NHE)	E^*, V (NHE)
I. $CO_2+2e^-+2H^+ \rightarrow H_2CO_2$	0	−0.19	−0.73*
	3	−0.36	−1.04
	4.7	−0.43	−1.23
	7.0	−0.47	−1.23
II. $H_2CO_2+2e^-+2H^+ \rightarrow H_2CO+H_2O$	0	−0.01	−0.99*
	2.5	−0.15	−1.16
	3.5	−0.21	−1.23
	7.0	−0.58	−1.27
III. $H_2CO+2e^-+2H^+ \rightarrow CH_3OH$	0	0.24	−0.97*
	3.5	0.04	−1.06
	5.0	−0.06	−1.11
	7.0	−0.17	−1.17
IV. $CH_3OH+2e^-+2H^+ \rightarrow CH_4+H_2O$	0	0.58	−0.87*
	7.0	0.17	−0.87

*Obtained by extrapolating the E^* (pH) relationships.

The facts that α_1 is constant over a large range of change in κ_1, which for ELH reactions on mercury reaches 10^{12}, and that α_1 increases from 0.5 to 1.0 at low overvoltages, have been explained quantitatively using a theoretical model developed by Benderskii and co-workers.[29,44–46] In this model, the view that there is a reorganisation of the polar medium on electron transfer is supplemented by taking account of the simultaneous quantum displacement of the proton.[47,48] Allowance for the inter-related movement of the proton and the medium leads to the following expression for the rate constant of hydrogen ion discharge:

$$\kappa_1 = \kappa_1^0 N_{H^+} \exp\left(-\frac{(E_s + E_p + \Delta G^0 - e(E_H^0 - E))^2}{4E_s kT + F^2\delta^2}\right), \quad (41)$$

where E_s and E_p are the energies of reorganisation along the coordinates of the medium and the proton respectively; δ the amplitude of the zero-point vibrations of the proton in the initial state; F the curvature of the proton term of the final state M−H; E_H^0 the potential of the normal hydrogen electrode (NHE); and κ_1^0 a pre-exponential term determined by the rate of tunnel electron transfer. According to Eqn. (41), the Tafel law applies for

$$e(E_H^0 - E) < E_s + E_p + \Delta G^0, \quad (42)$$

that is the reason for its applicability over a wide range of E is the high total energy (~3.3 eV, as shown below) of the reorganisation (the intramolecular reorganisation and that of the environment of the reaction complex).

The discharge becomes barrier-free when[46]

$$\Delta G^0 > E_s\left(1 - \frac{4kT}{h\omega}\right) + e(E_H^0 - E), \quad (43)$$

where ω is the frequency of the vibrations of the proton in the initial state. The theoretical model describes the change in $\kappa_1(E)$ in the range of both normal and barrier-free discharge, where the value of κ may change by a factor of more than 10^{18}. The values of E_s and E_p are 1.75 eV and 1.55 eV respectively. Thus the LPE method, which makes it possible for the first time to measure the absolute values of the rate constants of rapid ELH reactions, has led to the development of existing ideas on the mechanism of one of the most fundamental electrochemical processes.

VII. Intermediate species of the electrochemical carbon cycle

The electrochemical reduction of carbon dioxide to methane (the electrochemical carbon cycle) is an eight-electron process in which stable products: formic acid, formaldehyde, methanol, and methane, are formed at each of the successive two-electron stages. The redox potentials of these stages are given in Table 4. In acidic and neutral solutions in the absence of overvoltage, all the stages of the carbon cycle should have an appreciable rate even in the region of E_H^0. The overvoltage of stages (I) and (III), however, is greater than 1 V, and the reduction of H_2CO_2 and CH_3OH in aqueous solutions requires even higher overvoltages.[49] As in ELH reactions, the overvoltage is due to the formation of high-energy IS. An important role in the study of their electrochemistry was played by work[2,3,50–52] carried out by the PECR method, which established that for the radicals of the carbon cycle CHO, CH_2OH, and CH_3 there exists a fairly wide range of potentials in which the rate constants of the oxidation and reduction are lower than 10^3 s^{-1}. The relative electrochemical stability of the radicals and the weak pH dependence of the potentials of the polarographic waves of CH_3 and CH_2OH indicated that the products of the electrode reactions of the radicals are the high-energy organic ions CHO^-, CH_2OH^-, and CH_3^-, which then undergo homogeneous transformations into stable products (CH_2O, CH_3OH, and CH_4 respectively), whereas the exothermic electron−proton transfer reactions

$$R + e^- + H^+(aq) \rightarrow RH \quad (44)$$

take place at very low rates. The formation of CH_3^-, and not CH_4, in the reduction of CH_3 has been confirmed.[53] Calculation of the free energy of reactions (44) [2,54] also shows that the formation of HCO and CH_3 radicals cannot be responsible for the high overvoltage of stages (II) and (IV), that is the mechanism of the reactions of the carbon cycle is much more complex than a simple sequence of one-electron stages involving the formation and reduction of radicals. Low rates of reactions (44) have also been observed for many homogeneous processes associated with the formation of a CH bond with proton transfer.[55]

Each of the two-electron stages of the carbon cycle can be represented by the scheme

$$A \underset{W_2}{\overset{W_1}{\rightleftharpoons}} R \underset{W_4}{\overset{W_3}{\rightleftharpoons}} B, \tag{45}$$

which leads directly to the relationship between E^* and the standard potential B/A:

$$E^* = E^0 - \frac{kT}{e(\alpha+\beta)} \ln \frac{W_2^0}{W_3^0}, \tag{46}$$

where the rate constants of the electrode reactions of the radical W_2^0 and W_3^0 refer to the potential E^0 at which the two channels for the transformation of R have the same free energy. Since the rates of the transformation of the same species by two channels of equal energy under identical conditions cannot differ greatly, E^* and E^0 should be approximately equal. Thus by comparing the values of E^* and E^0 for the stages of the carbon cycle it is possible to establish whether the stable species listed in Table 4 are the products of the electrode reactions of the radicals.

The rate constants of the electrode reactions of the radical ion CO_2^- have been measured by the LPE method.[56,57] The $W_2(E)$ and $W_3(E)$ relationships are given in Fig. 10. The fact that the kinetic curves $Q(t)$ are exponential indicates that the electrode reactions involve adsorbed IS. Oxidation is observed at $E > -1.4$ V, W_2 is independent of pH and is equal to 3.5×10^6 s^{-1} at -1.35 V, and $\beta = 0.55-0.65$. Reduction takes place at $E < -1.5$ V, and $\alpha = 0.25-0.30$. The value of W_3 is linearly dependent on N_{H^+}. The participation of hydrogen ions in the reduction is confirmed by the marked isotope effect; the value of W_3 in H_2O solutions is three times that in D_2O. There is no isotope effect in the oxidation. The pH dependence of E^* is described by Eqns. (35) and (46);

for $W_{31}N_{H^+} \gg W_{30}$, the derivatives of $\frac{dE^*}{d\,pH} = -\frac{2.3}{\alpha+\beta}\frac{kT}{e}$,

and for $W_{31}N_{H^+} < W_{30}$ (pH $\geqslant$ 4.5), the potential E^* is constant. The polarograms obtained[53,56,57] for the CO_2^- ion generated by a low-frequency photo-emission current ($\Omega \ll W_2 + W_3$) give the sum of the transfer coefficients, which correspond to the values found by the pulse method.

According to Buxton and Sellers,[58] pK for the carboxyl radical HCO_2 is 1.4, so that in the solutions with pH $\geqslant$ 2.5 in which the LPE was measured, the IS are present as the radical ion CO_2^-. On adsorption on a negatively charged metal surface, the IS is apparently converted into the protonated form. The electrode reactions take place according to the equations:

$$HCO_2 \xrightarrow{W_2} CO_2 + H^+ + e^-,$$

$$HCO_2 + e^- + H^+ \xrightarrow{W_3} H_2CO_2. \tag{47}$$

At pH $\geqslant$ 4.5, water molecules become the main proton donors. From the numerical values of the constants found by the LPE method, it follows that in the region of E^* there is a change from the quasi-equilibrium reduction of CO_2 ($E > E^*$, $W_2 > W_3$) to ordinary reduction, and this change, in accordance with Eqn. (38), is in fact accompanied by a decrease in the effective transfer coefficient from $1 + \alpha$ to $1 - \beta$.[59] The measured[59] polarisation dependence of the current of the two-electron reduction of CO_2 coincides with the curves calculated from the LPE data using Eqn. (38). This means that the oxidation product of HCO_2 is CO_2. Comparison of the reduction current of CO_2, that is the values of κ_1, with W_2 made it possible, using Eqn. (40), to find the standard free energy of the reaction

$$CO_2 + e^- + H^+(aq) \rightarrow HCO_{2\,ads}, \tag{48}$$

equal to $\sim$154 kJ mol^{-1}. The coverage of the mercury surface by the radical does not exceed 10^8 particles cm^{-2}.

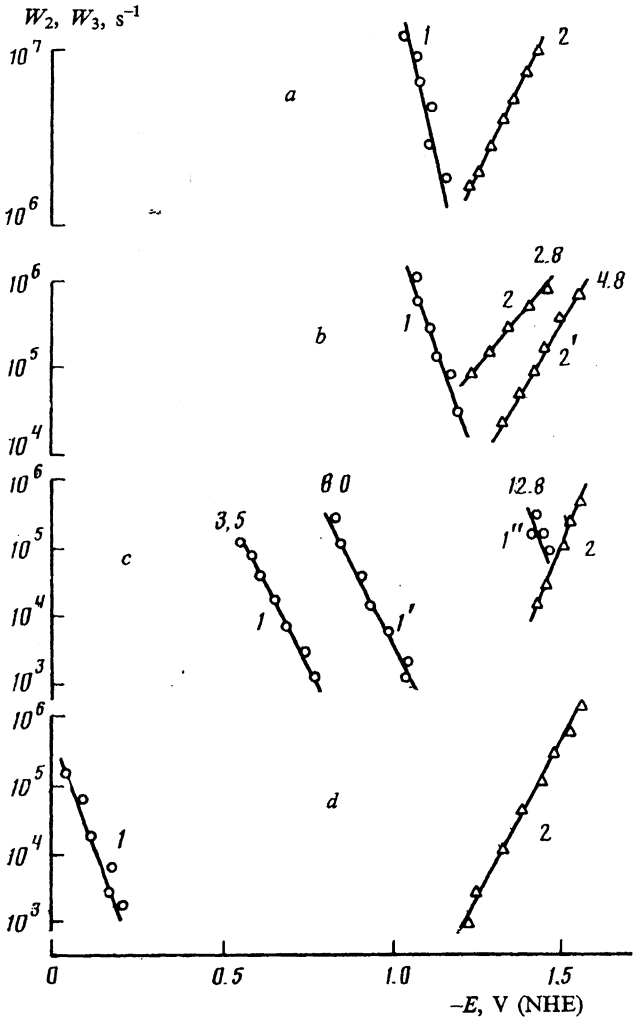


Figure 10. Tafel relationships for the rate constants of the oxidation (*1*, *1'*, *1''*) and reduction (*2*, *2'*) of the radicals CO_2^- (*a*), HCO (*b*), CH_2OH (*c*), and CH_3 (*d*) of the electrochemical carbon cycle at a mercury electrode; the pH values are given at the straight lines; for the other reactions, W_2 and W_3 are independent of pH.[54]

The electrode reactions of formyl radicals adsorbed on mercury have been studied.[60] As in the case of HCO_2, the rate constant for the oxidation of HCO [or its hydrated form $HC(OH)_2$] is independent of pH, and W_3 increases with decrease in pH, indicating that the reduction of the radical involves one hydrogen ion.

The values of W_2 and W_3 (Fig. 10) change from 10^4 s^{-1} (at $-E$ = 1.3–1.5 V) to 10^6 s^{-1} (at $-E$ = 1.5×1.8 V) (β = 0.45, α = 0.27). E^* changes in accordance with the pH dependence of W_3 (Table 4). At pH $\geqslant$ 4, the reduction involves water molecules, leading to a change in the transfer coefficient (α' = 0.35).

The difference $E^0 - E^*$ for the carboxyl and formyl radicals (Table 4) is such that it corresponds to a difference in W_2^0 and W_3^0 in Eqn. (46) by $10^{10}-10^{15}$. The unrealistic value of this difference indicates that the reduction of these radicals involves the formation of products with much higher energies than formic acid and formaldehyde. The fact that the reduction involves one electron and one proton shows that these species with higher energy must be isomers of these stable compounds. A high-energy isomer of formaldehyde is hydroxymethylene HCOH, formed, in particular, by the recombination of HCO and H after the photodissociation of H_2CO.[61] According to published data,[61,62] the energy of the ground state of HCOH is ~2.2 eV greater than that for H_2CO, so that the value of E^0 for the reaction

$$H_2CO_2 + 2H^+ + 2e^- \rightarrow HCOH + H_2O \qquad (49)$$

is close to –1.1 V and corresponds to the measured values of E^*. By analogy with the formyl radical, the product of the one-electron reduction of HCO_2 is apparently dihydroxymethylene $C(OH)_2$ [or its anion $C(OH)O^-$ in the reduction of CO_2^-]. These carbene derivatives subsequently undergo homogeneous isomerisation to H_2CO and H_2CO_2. Judging from a quantum-chemical calculation,[61] the barrier to the intramolecular rearrangement of *cis*-hydroxymethylene into H_2CO is ~50 kJ mol^{-1}, and the lifetime of HCOH in the gas phase is 4 μs.[63] The formation of carbene derivatives in electron–proton transfer reactions is consistent with the existing view that the hydrogen atom adds on to oxygen much more readily than to carbon.[55]

The methanol radical[64–66] is electrochemically much less active than HCO_2 and HCO; the constants W_2 and W_3 are 10^2-10^5 s^{-1} (Fig. 10). The rate constant for the reduction of CH_2OH adsorbed on mercury is independent of pH in the range 3–13, and remains unchanged when 1 M NH_4^+ ions as PD are added to the solution. The transfer coefficient for W_3 is 0.68. Unlike W_3, the rate of oxidation increases sharply with increase in pH, and change in pH also leads to a change in the transfer coefficient. In the pH range 3.5–7, β = 0.63, and the displacement of E with change in pH at constant W_2 (dE/dpH) is ~0.06 V. In the pH range 8–12, β = 0.3, and dE/dpH $\simeq$ 0.16, corresponding to a first order reaction with respect to OH^- ions. At pH $\geqslant$ 12.5, at which the radical is present in the ionic form (pK = 10.6[3]), W_2 is independent of pH, and β = 0.5. The dependence of W_2 and W_3 on pH and E corresponds to the reactions

$$CH_2OH + OH^- \rightarrow CH_2O + H_2O + e^-,$$
$$CH_2OH + e^- \rightarrow CH_2OH^-. \qquad (50)$$

At pH $\leqslant$ 8, water molecules act as hydrogen acceptors in the oxidation of the radical. Because of the relatively low values of W_2 and W_3, the surface concentration of the radical increases to such an extent that its electrode reactions can be detected by ordinary electrochemical methods, in particular by the cyclic voltammetric study of formaldehyde solutions. The $\Gamma(E)$ relationships calculated using Eqn. (39) from the polarisation curves for the reduction of H_2CO[49] are given in Fig. 11. They agree with published data;[49,67,68] appreciable accumulation of the radical is observed in the pH range 6.8–9.0, and is not recorded in more alkaline solutions. The position and height of the maxima of the anodic current on the voltammetric curves[67,68] coincide with those calculated from the measured[66] constants W_2 and W_3. The published[66] comparison of the LPE and cyclic voltammetric data shows that the IS generated in photo-emission and in the reduction of CH_2O are identical. In both cases the IS is CH_2OH. The fact that W_3 is independent of pH, indicating that hydrogen ions do not take part in the reaction, the high transfer coefficient, characteristic of endothermic reactions, and the large difference in the potentials E^* and E^0 for the formation of CH_3OH from CH_2O (Table 4) show that the reduction product of formaldehyde is the carbanion CH_2OH^-, and not methanol. The calculated[69] energy of the tautomerisation of the methoxide ion CH_3O^- into CH_2OH^- is ~93 kJ mol^{-1}. The potential E^0 for the reaction

$$CH_2O + 2e^- + H^+ \rightarrow CH_2OH^-(aq), \qquad (51)$$

calculated from this value and pK for CH_3OH, agrees with the measured value of E^*. The free energy of the adsorption of CH_2OH on mercury is –40 kJ mol^{-1},[66] and for HCO_2, ΔG_a = –44 kJ mol^{-1}.[56]

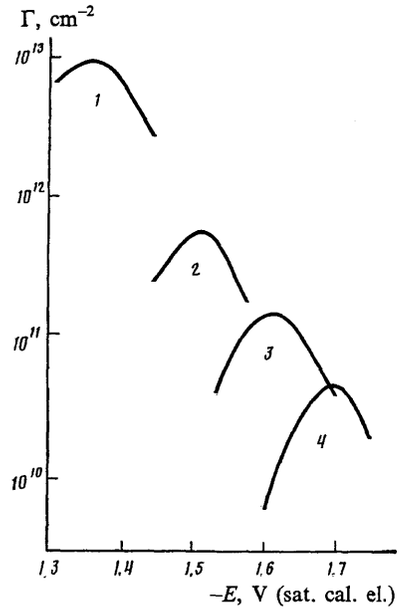


Figure 11. Surface concentration of the CH_2OH radical in the reduction of formaldehyde at a mercury electrode at different pH values: *1*, 6.8; *2*, 9.0; *3*, 11.1; *4*, 13.0.[66]

The reduction of CH_3 also takes place without the participation of PD, and leads to the formation of the CH_3^- anion, whose free energy has been calculated.[3]

The diagram of the free energies of the successive one-electron reactions of the electrochemical carbon cycle, based on the values of E^* given in Table 4 for stages (I)–(III) and the thermodynamic characteristics of the free radicals,[70] is given in Fig. 12. In a neutral

solution, the free energy of the overall process

$$CO_2 + 8\,H_2O + 8\,e^- \rightarrow CH_4 + 8\,OH^- \qquad (52)$$

is 204 kJ mol^{-1}. The additional energy losses at each of the two-electron stages are due to the transformation of the reduction products of the radicals $C(OH)_2$, HCOH, CH_2OH^-, and CH_3^- into H_2CO_2, H_2CO, CH_3OH, and CH_4 respectively, and amount to 755 kJ mol^{-1}. From this it follows that the energetic efficiency of the electrochemical carbon cycle does not exceed 21%. Since the energy losses are due to the formation of the carbanions CH_2OH^- and CH_3^-, which are not adsorbed on the negatively charged electrode surface, the efficiency of the corresponding stages is the same for different metals. Thus even the energy efficiency (without allowance for current losses) of the sequence of one-electron reactions being considered is extremely low, so that it is important to find catalytic electrochemical systems in which either two-electron transfer without the intermediate formation of radicals or simultaneous electron transfer and proton addition with the formation of a CH bond are possible.

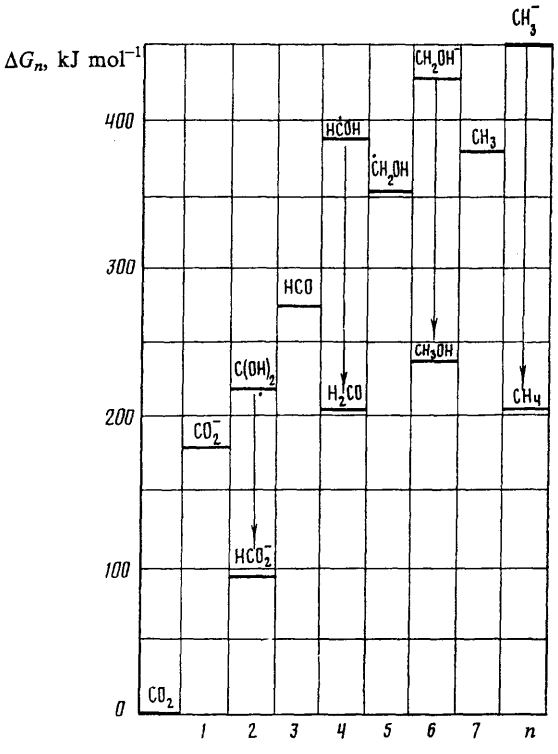


Figure 12. Free energies of the reactions of the electrochemical carbon cycle at pH 7.

VIII. Electrochemistry of alkyl and hydroxyalkyl radicals

Alkyl radicals are IS in the two-electron reduction of alkyl halides;[71] they are also formed in the one-electron reduction of alkylmercury compounds.[72,73] The PECR method gave the polarograms of CH_3 at a mercury electrode 10^{-5} s after a radiolysis pulse, and detected a wide range of potentials in which the CH_3 radical is electrochemically inactive.[2] It has been suggested that the reduction product of CH_3 is the carbanion CH_3^-, and not methane.[2,53,72,73] The rate constants of the electrode reactions of alkyl radicals could not be measured by electrochemical methods, since their recombination is a multi-stage process. It has been suggested[72,74] that the formation of HgR_2 is preceded by the rapid formation of the organic calomel Hg_2R_2, capable of dissociation, and that the radicals are present on the mercury surface as HgR. The rate constants of the heterogeneous reactions of these radicals have been measured by the LPE method.[24] In the working range of the mercury electrode ($E < -0.1$ V), only the oxidation of CH_3 is observed. The Tafel straight lines $\ln W_3(E)$ are displaced to more negative values of E in the series CH_3, C_2H_5, n-C_3H_7, n-C_4H_9. There exists a wide range of E (for CH_3, for example, from -0.6 V to -1.3 V) in which there are no IS electrode reaction currents, that is the rates of these reactions are lower than the rate of surface recombination. An analysis of the polarograms recorded at different Ω gave the rate constants of the last process, which takes place according to the scheme

$$\begin{array}{ccccc} CH_3Hg^+ & \overset{W_2}{\leftarrow} & CH_3Hg & \overset{W_3}{\rightarrow} & CH_3^- + Hg^+ \\ & & \gamma\downarrow \quad \uparrow k_2 & & \\ & & (CH_3)_2Hg_2 & \overset{k_3}{\rightarrow} & (CH_3)_2Hg \end{array} \qquad (53)$$

with $\gamma = 5 \times 10^{-9}$ cm^2 s^{-1}, $k_2 = 3 \times 10^2$ s^{-1}, $k_3 \simeq 20$ s^{-1}. The values of the constants correspond to the cyclic voltammetric curves for the radical.[73] The surface concentrations of the radical (Γ_R) and the dimer (Γ_d) in the kinetic scheme (53) are:

$$\Gamma_R = \frac{W}{2m\gamma}\left(\sqrt{1+\frac{4mj_R}{W^2}}-1\right), \quad \Gamma_d = \frac{m\gamma}{k_3}\Gamma_R^2, \quad m = \frac{k_3}{k_2+k_3}, \qquad (54)$$

where j_R is the current of the electrochemical or photo-emission formation of CH_3. In the range in which the radical is electrochemically stable ($W < \gamma\Gamma_R$), the adsorbate exists chiefly as the dimer ($\Gamma_d \gg \Gamma_R$). When the rate of the electrode reactions increases to such an extent that $W > \gamma\Gamma_R$, the concentrations Γ_R and Γ_d decrease, and $\Gamma_R > \Gamma_d$. During the cyclic scanning of the potential in the range corresponding to the reduction of RHg^+, the dimer accumulates, and the limiting stage of the reduction at $E \leqslant -1.3$ V becomes its decomposition to radicals with rate constant k_2.

According to PECR data,[50,75] the α-ethanol radical CH_3CHOH, which is an IS in the reduction of acetaldehyde, is oxidised with a rate constant W_2 which decreases from 10^5 s^{-1} to 10^4 s^{-1} in the range of E values from -1.0 V to -1.3 V. The $W_2(E)$ and $W_3(E)$ relationships for this radical, measured by the LPE method,[21,76] are similar to the corresponding relationships for the CH_2OH radical (see Fig. 10). The reduction rate constant W_3 is independent of pH. The $W_3(E)$ relationships measured in the range $10-10^3$ s^{-1} and 10^4-10^5 s^{-1},[75,76] lie on the same Tafel straight line, and in this case the transfer coefficient α is 0.5. The constant W_2 increases with pH at pH > 8, in agreement with the fact that the oxidation is first order with respect to OH^- ions [see Eqn. (50)]. At pH < 7, the constant W_2 is independent of the acidity, that is the radical is oxidised to the aldehyde with the formation of a hydrogen ion.

The $W_2(E)$ and $W_3(E)$ relationships for the isopropyl alcohol radical at different pH values (Fig. 13) show that the oxidation and reduction of this radical take place by the same mechanism as the transformations of CH_2OH and CH_3CHOH. Studies of the electrochemical reduction of acetone[77,78] have shown that the adsorbed radical $(CH_3)_2COH$ is the IS in this process.

At $E > -1.3$ V, the formation of the radical in acidic solutions takes place in quasi-equilibrium fashion ($W_2 > W_3$), so that under the conditions of a cyclic increase in E, the IS is oxidised almost quantitatively to acetone. The absolute values of W_2, measured by the potential jump method,[77] increase from 10^4 s^{-1} to 4×10^4 s^{-1} with increase in E from –1.3 V to –1.23 V ($\beta = 0.5$). The formation of the radical in the reduction of acetone is a first-order reaction with respect to hydrogen ions. The order of magnitude of the values of W_2 measured by the LPE method agrees with that of published data;[77] the β values also coincide. A quantitative comparison of the results obtained by these two methods is difficult, because of the difference in the pH and acetone concentrations at which the measurements were carried out (pH < 1 and $N_a \simeq 4$ M in the study of Brown and Lister,[77] and pH $\geqslant$ 4 and $N_a \leqslant 0.5$ M in the LPE measurements). Since acetone and the radical are adsorbed on mercury, the values of W_2 correspond to different degrees of coverage of the surface. The values of W_3 measured by LPE and low-frequency photoemission methods[21,64] at pH $\geqslant$ 4 are smaller by factors of $10^3 - 10^4$ than those corresponding to the current for the reduction of acetone to isopropyl alcohol at pH $\leqslant$ 1.[77] This difference indicates that in strongly acidic solutions, the reduction of the radicals involves hydrogen ions:

$$(CH_3)_2COH + e^- + H^+ \rightarrow (CH_3)_2CHOH, \quad (55)$$

whereas at pH $\geqslant$ 4, as in the case of CH_2OH and CH_3CHOH, the reduction product is the carbanion $(CH_3)_2COH^-$. With two parallel channels for the quasi-equilibrium formation of the radical, the reduction current of acetone is given by the relationship

$$j_0 = 2e\Gamma_0 \frac{W_1}{W_2} N_{H^+}(W_{30} + W_{31}N_{H^+}), \quad (56)$$

where Γ_0 is the surface concentration of acetone, and W_1 the rate constant for its reduction to the radical, equal to 3×10^2 s^{-1} at $E = -1.28$ V in 0.5 M H_2SO_4 solution ($\alpha_1 = 0.5$).[77] It follows from Eqn. (56) that $j_0 \sim N_{H^+}^2$ when $W_{31}N_{H^+} > W_{30}$, in agreement with published data.[78] Comparison of the values of W_{30} and W_{31} measured by the LPE and potential jump methods shows that at pH 3, $W_{31}N_{H^+} \simeq W_{30}$. In alkaline solutions, the main reduction product of acetone is pinacone, which, as suggested as early as 1927,[79] is formed either by the bimolecular recombinations of the radicals or by the reaction of acetone with the carbanion. With increase in pH, the rate constant W_2 increases, and the reduction of acetone takes place at more negative potentials, at which, as a result of the increase in W_3, the concentration of the radical decreases [see Eqn. (39)], as in the case of the methanol radical (see Fig. 10). The decrease in Γ with increase in pH does not agree with the first of these mechanisms, whereas with increase in W_3, which indicates an increase in the rate of formation of the carbanions, it is possible to explain the increase in the yield of pinacone in alkaline solutions.

According to PECR [2,3] and LPE data, the reduction of the β-ethanol radical CH_2CH_2OH involves one hydrogen ion:

$$CH_2CH_2OH + e^- + H^+ \rightarrow C_2H_4 + H_2O. \quad (57)$$

The values of W_3 change from 10 s^{-1} to 10^5 s^{-1} in the range of E values from –0.65 V to –1.34 V at pH 5.5 ($\alpha \simeq 0.4$). The marked displacement of the reduction potential of the radical into the cathodic range compared with the expected potential for the production of ethylene according to Eqn. (57), for which the free energy is –131 kJ mol^{-1}, indicates that the reaction product is the adsorbed biradical CH_2-CH_2. This is consistent with the high overvoltage observed in the electrochemical synthesis of cycloalkanes from their dihalogeno-derivatives,[71] taking place at $E \leqslant -2.0$ V.

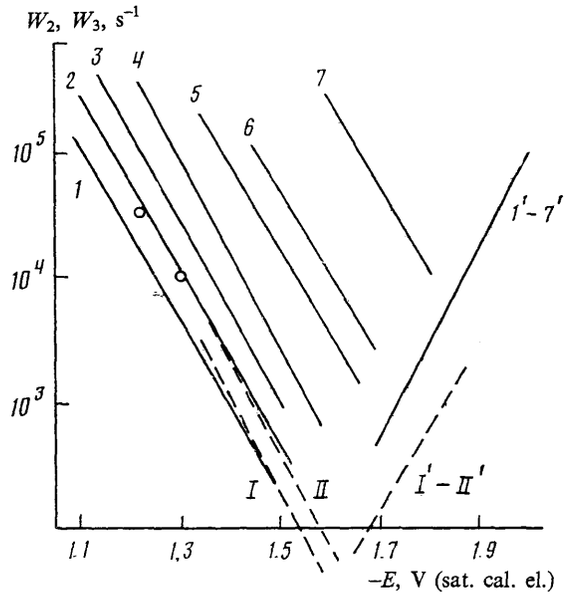


Figure 13. Tafel relationships for the rate constants of the oxidation (*1–7*) and reduction (*1'–7'*) of the isopropyl alcohol radical adsorbed on a mercury electrode at different pH values: *1, 1'*, pH 4.25; *2, 2'*, pH 6.8; *3, 3'*, pH 7.35; *4, 4'*, pH 8.1; *5, 5'*, pH 9.15; *6, 6'*, pH 10.0; *7, 7'*, pH 10.8; the points give the values measured by Brown and Lister,[77] and the broken lines the data of Rotenberg and Rufman;[64] the straight lines *I* and *I'* were obtained at pH 4.6, and *II* and *II'* at pH 7.0.

Mairanovskii[80] has suggested that there is no protonation with the formation of a CH bond in the electrode reactions of organic compounds. The opposite view was put forward by Elving,[81] who considered that the reduction of organic compounds is analogous to the electrochemical desorption of hydrogen.

The above data obtained by the LPE method, which has made it possible for the first time to measure systematically the rate constants of the electrode reactions of simple alkyl and hydroxyalkyl radicals, provide clear evidence in support of the first suggestion. Even in the reduction of the $(CH_3)_2COH$ radical in acidic solutions, where it was possible to observe the electron–proton transfer reaction (55), its rate constant was 10^6 times smaller than the rate constant for electrochemical desorption (Table 3). For other radicals, W_{31} is even smaller. The diagram in Fig. 12 makes it possible to estimate quantitatively the difficulty of protonation with the formation of a CH bond. For example, the exothermic formation of methane from the methyl radical takes place at a lower rate than the endothermic formation of the CH_3^- ion, although ~180 kJ mol^{-1} is liberated in the first reaction, whereas 75 kJ mol^{-1} is used up in the second. The CH_2OH^- and CH_3CHOH^- anions are formed instead of methane and ethanol, despite the fact that the free

energies of formation of these carbanions from the radicals are ~170 kJ mol^{-1} greater than those for the alcohols. Thus the barrier associated with the reorganisation of the the complex in the transfer of a proton with the formation of a CH bond for simple organic radicals is greater than 150–200 kJ mol^{-1}. Since the rates of protonation with the formation of an OH bond are much higher, carbene derivatives are formed in the reduction of carboxyl radicals.

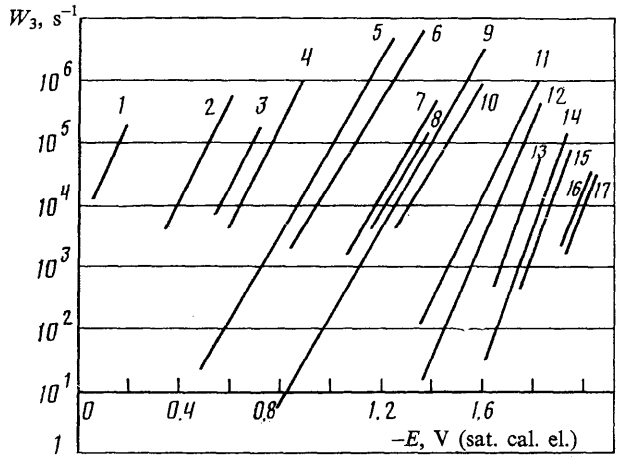


Figure 14. Tafel relationships for the rate constants of the reduction of simple organic radicals to carbanions:[82] *1*, CCl_3; *2*, CCl_2F; 3, $CClF_2$; *4*, CF_3; *5*, $CHCl_2$; *6*, CHFCl; *7*, CHF_2; *8*, C_6Cl_5; 9, CH_2Cl; *10*, C_6H_5; *11*, CH_3; *12*, CH_2OH; *13*, C_2H_5; 14, C_2H_4OH; *15*, $(CH_3)_2COH$; *16*, n-C_3H_7; *17*, n-C_4H_9.

IX. The p*K* scale for weak CH-acids

The rate constants for the one-electron reduction of a number of simple organic radicals to carbanions have been measured by the LPE method.[82] The $W_3(E)$ relationships for all the radicals studied have similar values of the transfer coefficient $\alpha = 0.45 \pm 0.05$ (Fig. 14). An empirical rule was proposed[82] for relating the potentials of the Tafel straight lines $\ln W_3(E)$ to the energy characteristics of the carbanions: the displacement of the standard redox potential E^0 of the reaction

$$R + e^- \rightarrow R^- \qquad (58)$$

for a series of organic radicals is equal to the displacement of the potential corresponding to identical values of W_3. The equation for the retarded discharge can be written as:

$$\ln W_3 = \ln W_3^0 - \frac{E_a^0}{RT} - \alpha\frac{\Delta G_a^0}{RT} + \alpha\frac{E}{RT}(E^0 - E), \qquad (59)$$

where E_a^0 and W_3^0 are respectively the activation energy and the pre-exponential term for $E = E^0$. In Eqn. (59), allowance has been made for the fact that the radical is present in the adsorbed state. It follows from Eqn. (59) that the relative displacement of the Tafel straight lines along the E scale for equal values of W_3 and α is related to the difference in E^0 by the expression

$$\Delta E_{12} = \Delta E_{12}^0 - \frac{RT}{\alpha F}\ln\frac{W_{31}^0}{W_{32}^0} - \frac{1}{\alpha F}(E_{a_1}^0 - E_{a2}^0) - \frac{1}{F}(\Delta G_{a1}^0 - \Delta G_{a2}^0). \qquad (60)$$

According to Eqn. (60), the rule formulated above ($\Delta E_{12} = \Delta E_{12}^0$) applies if the transfer coefficients of the radicals, the pre-exponential terms, the activation energies E_a^0, and the free energies of adsorption coincide. It has been established experimentally that α is constant. The fact that E_a^0 and W_3^0 coincide is a direct consequence of the model of electron transfer in a polar medium;[47,48] according to this model, W_3 characterises the probability of electron transfer from the metal to the reaction complex, and $E_a^0 = E_s/4$ (E_s is the energy of reorganisation of the medium in this transfer). The requirement that ΔG_a^0 be constant, which means the preservation of the energy of the M–C bond in the series of radicals, is the least rigid of the above conditions, since this quantity is comparatively small ($\leqslant 50$ kJ mol^{-1}).

From the empirical rule and the measured values of $W_3(E)$, it is possible to compile a scale of relative values of E^0. To change to the absolute scale, the standard potentials of the following reactions were calculated[82]

$CH_3(gas) + e^- \rightarrow CH_3^-(aq)$ and
$CH_2OH(gas) + e^- \rightarrow CH_2OH^-(aq)$:

$$E^0 = \frac{F}{RT}(\Delta G_{R^-}^0 - \Delta G_R^0) = \frac{F}{RT}(\Delta G_h^0 - EA - \Delta G_{H^+}^0 - RT\ln 24{,}5), \qquad (61)$$

where ΔG_h^0 is the hydration energy of R^-, EA the electron affinity of the radical in the gas phase, and $\Delta G_{H^+}^0 = -430$ kJ mol^{-1} the standard free energy of hydration of the proton, used to change from the energy scale in a vacuum to the energy scale in aqueous solution. The last term in Eqn. (61) takes account of the difference between the standard states of the ion in the gas and in solution. The value $\Delta G_h^0 = -322$ kJ mol^{-1} for CH_3^-, taken as equal to the hydration energy of the hydride ion,[2] is close to the values of ΔG_h^0 for the NH_4^+ and K^+ ions (−314 kJ mol^{-1} and −330 kJ mol^{-1} respectively), which have approximately the same dimensions. The electron affinity of the methyl radical is 7.7 ± 2.9 kJ mol^{-1},[83] so that the free energy of the CH_3^- ion in water is 230 ± 16 kJ mol^{-1} and $E^0 = -0.77 \pm 0.16$ V. The calculated energy of the ground state of the CH_2OH^- ion is 93 kJ mol^{-1} greater than the energy of CH_3O^-.[84] Using the value of pK (CH_3OH) and assuming that the solvation energies of the two ions are equal, it is found that for $CH_2OH^-(aq)$, $\Delta G^0 \simeq 60$ kJ mol^{-1}, and $E^0 = -0.85$ V. The difference in E^0 for these two reactions corresponds to the displacement of the Tafel curves. The free energies of the other carbanions are given by the expression

$$\Delta G_{R^-}^0 = \Delta G_{R_0^-}^R + \delta(\Delta G_{CH}^0) + \frac{RT}{F}\Delta E^0, \qquad (62)$$

where $\Delta G_{R_0^-}^0$ is the free energy of the "standard" carbanion CH_3^-, and $\delta(\Delta G_{CH}^0)$ the difference between the free energies of the rupture of the CH bond in R_0H and RH. In Eqn. (62), the difference in the hydration energies of R and RH is not taken into account. The free energies of different carbanions are given in Table 5, which also gives the values of E^0 and pK for the CH-acids conjugate with R^-:

$$pK = \frac{1}{2{,}3RT}(\Delta G_{R^-}^0 - \Delta G_{RH}^0), \text{ where } \Delta G_{RH}^0 \text{ is the free energy of RH.}$$

The pK scale defines the relative reactivity of organic substances in nucleophilic substitution reactions.[85] Several methods have been proposed for constructing it from indirect data, in particular from the rate constants of proton exchange.[86] Attempts have been made to determine the pK values by semi-empirical quantum-chemical calculations.[87] The most universal is the polarographic pK scale, constructed using the half-wave potentials for the two-electron

reduction of the symmetrical organomercury compounds HgR_2 to the carbanions in non-aqueous solvents.[88] It was assumed[88] that the reduction of HgR_2 takes place under conditions close to equilibrium, and that the change in $E_{1/2}$ corresponds to the displacement of pK. Because of the complexity of the two-electron process, indicated, for example, by the above data on the reduction of CH_3Hg^+ to CH_3^-, this approximation is less obvious than that used by Benderskii and co-workers.[82] The values of pK found by different methods sometimes differ by factors of $10^{10}-10^{12}$.[88] For comparison, it may be noted that even a difference by factors of 10^3-10^4 in the pre-exponential terms in Eqn. (60) leads to a scatter in the relative values of pK of 5–7 units. The pK values for the haloforms CHF_3 and $CHCl_3$ found by the published methods[88,82] coincide.

Table 5. Free energies of organic radicals (ΔG^0_R) and carbanions ($\Delta G^0_{R^-}$, aq), standard redox potentials E^0 of the formation of the carbanions from the radicals, and the pK values of CH-acids RH.[82]

Radical	ΔG^0_R, kJ mol^{-1}	ΔG^0_R, kJ mol^{-1}	$-E^0$, V	CH-Acid	pK
CH_3	145	(230)	(0.77)	CH_4	(47)
C_2H_5	139	247	0.95	C_2H_6	48.5
n-C_3H_7	148	263	1.18	**n-C_3H_8**	49.6
n-C_4H_9	160	276	1.19	**n-C_4H_{10}**	50.8
CH_2OH	—18	60	0.85	CH_3OH	40.8
CH_3CHOH	39	61	1.01	C_2H_5OH	42
$(CH_3)_2COH$	26	73	1.04	$(CH_3)_2CHOH$	42.7
CH_2Cl	122	176	0.42	CH_3Cl	39.5
$CHFCl$	—85	—49	0.12	CH_2FCl	31.7
CHF_2	—237	—203	0.36	CH_2F_2	37.3
$CHCl_2$	95	98.5	0.04	CH_2Cl_2	31.2
CF_2Cl	—269	—295	—0.26	CHF_2Cl	23.2
$CFCl_2$	82	—122	—0.44	$CHFCl_2$	19.9
CF_3	—456	—283	—0.18	CHF_3	29.7
CCl_3	95	19.1	—0.79	$CHCl_3$	15.2
C_6H_5	349	397	0.49	C_6H_6	46.2
C_6Cl_5	—	—	0.42	C_6HCl_5	38

The pK values for CH-acids in the gas phase have been found by measuring the electron affinity of the radicals by the ion-cyclotron resonance method.[89,90] Although these data are extremely convenient for determining the influence of different substituents on pK, they cannot be used to construct the pK scale for solutions, since the differences in the solvation energies of the carbanions mask the changes in acidity associated with the introduction of the substituents. For example, the pK values for the CH-acids CH_4 and CHF_3 differ by 29 units in the gas phase,[89] and by 17 units in aqueous solution, that is the difference ΔG^0_t is 69 kJ mol^{-1}.

The pK scale in solutions is not universal, since the change to another medium changes $\Delta G^0_{R^-}$ by an amount equal to the free energy of the transfer of the carbanion between the solvents ΔG^0_t. For inorganic ions, the value of ΔG^0_t lies in the range 10 to 25 kJ mol^{-1}.[91] In the method of Benderskii and co-workers,[82] change in the solvent leads to additional errors due to the relative changes in the energy of reorganisation. Measurements of $W_3(E)$ for CH_2Cl and $CHCl_2$ radicals in acetonitrile and water–dioxan mixtures showed that the displacement of the Tafel curve does not exceed 0.15 V, that is the difference in the relative values of pK in these solvents and in water is less than 5 units. It should be emphasised that the method[82] is universal, and does not lose its accuracy with increase in pK, and the range in which measurements can be made corresponds to the working range of potentials of the mercury electrode, and is greater than 30 pK units.

The range of change in W_3 in which the $W_3(E)$ relationships were measured for the CH_2Cl and $CHCl_2$ radicals[16] is greater than 10^6 (Fig. 14). The deviations from the Tafel law predicted by the theory of electron transfer in a polar medium[47,48] were not detected in this range. According to Marcus' model, the transfer coefficient for outer-sphere reactions in the range of normal discharge is a linear function of the overvoltage:

$$\alpha = \frac{1}{2} - \frac{e}{2E_s}(E^0 - E), \quad |e(E^0 - E)| < E_s. \tag{63}$$

Eqn. (63) shows that at $E_s \leqslant 200$ kJ mol^{-1}, corresponding to ELH reactions (see section IV), α should decrease from 0.5 to 0.30–0.25 in the measured range of E, but this does not agree with experiment. It was previously concluded from an analysis of the polarisation relationships in simple electrode reactions[92,93] that Eqn. (63) does not agree with experiment. The data of Benderskii and co-workers[16] confirm this conclusion; for the fulfilment of the Tafel law to agree with Eqn. (63), it is necessary to assume that $E_s \gtrsim 300$ kJ mol^{-1}, which is comparable with the solvation energy of the carbanions. This is contrary to the concept of a linearly polarised medium[94] on which the theory is based.[47,48] Benderskii and co-workers[16] suggested that the electron transfer is associated not only with reorganisation of the medium but also with reorganisation of the reaction complex itself. In the initial state, the adsorbed radical is in the compact part of the electrical double layer, where the water molecules are oriented by a strong electric field and cannot solvate the carbanion formed by electron transfer. Thus the solvation of the reaction product involves a displacement of the reagent along the adsorption coordinate in the direction of the Helmholtz plane. The existence of this reaction coordinate, associated with the desorption of the radical, which is necessary for solvation in the transition state, leads to the appearance of an additional energy of reorganisation. The combination of these two movements (of the radical and the medium) is similar to that examined[45] for ELH reactions, and leads to the relationship

$$\ln\frac{W_3}{W_3^0} = -\frac{(E_s + E_1 - e(E^0 - E))^2}{4E_s kT + rF^2\delta^2}, \tag{64}$$

where E_1 is the energy of reorganisation of the adsorbed radical, F the curvature of the carbanion term, $r^{-1} = 2\tanh(\hbar\omega/2kT) - 1$, and δ and ω are respectively the amplitude and frequency of the vibrations in the initial state. Eqn. (68) agrees with experiment for $E_1 \simeq E_s$. The value $E_s \simeq 150$ kJ mol^{-1} corresponds to the energy of reorganisation of the medium in the one-electron reduction of NO to NO^- (see section X), and explains why pK changes little with change in the solvent.

X. Intermediate species of the electrochemical nitrogen cycle

The electrochemical reduction of NO_3^- ions to NH_3 (the electrochemical nitrogen cycle) is an eight-electron process including the electronic stages of the formation of NO_2^- from NO_3^- ($n = 2$), NO from NO_2^- ($n = 1$), NH_2OH from NO ($n = 3$), and NH_3 from NH_2OH ($n = 2$). Each of these stages is associated with the transformation of short-lived IS: NO_3^{2-}, NO_2^{2-}, NO^-, H_2NO, and NH_2. Although the existence of these IS in aqueous solutions was

established by pulse radiolysis and EPR methods, their role in the nitrogen cycle was revealed only recently, by the LPE method.[95–98] The results are summarised in Fig. 15, and the rate constants of the homogeneous and electrode reactions of the IS are given in Tables 6 and 7.

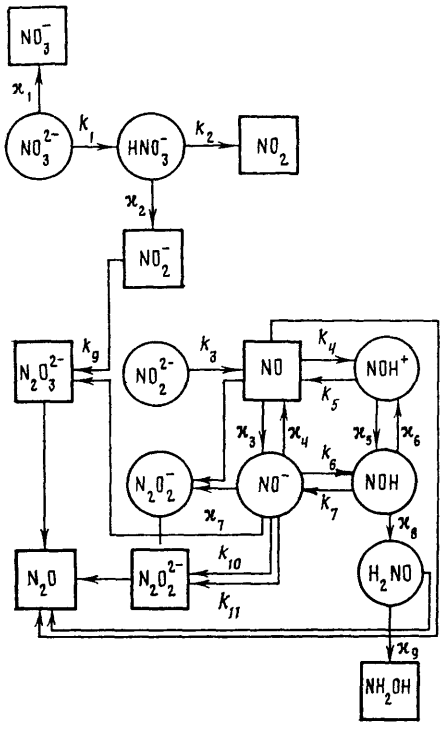


Figure 15. Homogeneous and electrode reactions of the IS of the electrochemical nitrogen cycle.

Table 6. Rate constants of the homogeneous reactions of the IS of the electrochemical nitrogen cycle.[96–98]

Reaction	K, mol^{-1} s^{-1}	Reaction	K, mol^{-1} s^{-1}
$NO_3^{2-}+H_2O \rightarrow HNO_3^-+OH^-$	$1\cdot10^3$	$NO^-+NH_4^+ \rightarrow NOH+NH_3$	$\sim10^6$
$NO_3^{2-}+NH_4^+ \rightarrow HNO_3^-+NH_3$	$2\cdot10^8$	$NO^-+H^+ \rightarrow NOH$	$\sim10^{10}$**
$NO_3^{2-}+H^+ \rightarrow HNO_3^-$	$2\cdot10^{10}$	$NO^-+NO \rightarrow N_2O_2^-$	$2\cdot10^9$
$HNO_3^- \rightarrow NO_2+OH^-$	$2.3\cdot10^5$*	$NO^-+NO_2^- \rightarrow N_2O_3^{2-}$	$\sim10^8$
$NO_2^{2-}+H_2O \rightarrow NO+2OH^-$	$9\cdot10^4$	$NO^-+NO^- \rightarrow N_2O_2^{2-}$	—
$NO+NH_4^+ \rightarrow NOH^++NH_3$	$\geqslant10^4$	$NOH \rightarrow NO^-+H^+$	$\sim10^6$*
$NOH^+ \rightarrow NO+H^+$	$>10^6$*	$H_2NO+NO \rightarrow H_2N_2O_2$	$\sim10^8$

* Unimolecular constant with dimensions s^{-1}. ** Estimate based on the value pK = 4.7 [99] and the rate constant of the dissociation of NOH.

Table 7. Rate constants of the electrode reactions of the IS of the electrochemical nitrogen cycle.[96–98]

Reaction	$-E$, V (NHE)	κ, cm s^{-1}	Transfer coefficient
$NO_3^{2-} \rightarrow NO_3^-+e^-$	0.76	1.5	0.25
$HNO_3^-+e^- \rightarrow NO_2^-+OH^-$	>0.8	$\geqslant$10	—
$NO+e^- \rightleftharpoons NO^-$	0.81	2	0.50
$HNO+e^-+NH_4^+ \rightarrow H_2NO+NH_3$	>1.0	>1	—
$H_2NO+e^++NH_4^+ \rightarrow NH_2OH+NH_3$	>1.0	>1	—

The product of the capture of e^-_{aq} by the nitrate ion is oxidised on mercury with a rate constant which increases from 0.1 cm s^{-1} to 10 cm s^{-1} with change in E from −1.2 V to −0.9 V (β = 0.25).[9] The oxidation competes with the homogeneous decompostion of the IS, for which the characteristic time is 1.3×10^{-5} s and 3×10^{-6} s for NO_3^{2-} and HNO_3^- respectively.[100] The decomposition product in the one-electron process is reduced. The charge of the IS oxidised was established[95] from the kinetic ψ_1-effect. At $\psi_1 < 0$, the electric field of the diffuse double layer retards the movement of the negatively charged IS towards the electrode. Since they have a finite lifetime in solution, this retardation increases the proportion of IS decomposing, compared with the proportion oxidised at the electrode, leading to an increase in the current and potential of the anodic half-wave of the IS. Analysis of the equations for the diffusion in the field of the ψ_1 potential of e^-_{aq} and the IS being oxidised leads to the relationship

$$j_1 = 2\frac{j-j_{\min}}{2-j_{\min}} = \left(1+\varkappa\sqrt{\frac{\tau}{D}}e^{-\Phi}+\frac{\varkappa x_0}{D\Phi}\right)^{-1}, \qquad (65)$$

where $j_{\min}$ is the minimum value of the current, corresponding to $\kappa \rightarrow \infty$, κ the rate of oxidation of the IS, τ the decomposition time of the IS, x_0 the characteristic dimension of the diffuse double layer, and $\Phi = \frac{eZ}{kT}\psi_1$, where Z is the charge of the IS. The second term in the denominator of Eqn. (65) characterises the ratio of the rates of the electrode reaction to the diffusion of the IS to the electrode under the condition of Boltzmann equilibrium, and leads to the Frumkin relationship[27]

$$\Delta E_{1/2} = (1+Z/\beta)\Delta\psi_1 \qquad (66)$$

which gives the dependence of the displacement of the half-wave potential of the species stable in solution on the ψ_1-potential. The third term, equal to the ratio of κ on the rate of the drift of the IS from the electrode into the solution, takes account of the deviation from equilibrium in strong fields, when the ψ_1-effect is due to the above-mentioned retardation of the IS. Eqn. (66) is applicable when $|\Phi| < \Phi^*$, where Φ^* is the solution of the equation $\Phi^*\exp(-\Phi^*) = x_0/\sqrt{D\tau}$, so that the applicability of the Frumkin equation depends on the lifetime of the IS in solution. The measured[95] displacement of the anodic wave in solutions with different ionic strengths, in which the ψ_1-potential changed from 0 to 0.09 V, corresponds to $Z = -2$, that is the primary IS is the NO_3^{2-} ion. It follows from the kinetic LPE curves that the characteristic time of the reduction of the product of the transformation of NO_3^{2-} does not exceed 2×10^{-7} s. The absence of an arrest corresponding

to the lifetime of HNO_3^- means that the decomposition of this ion (to give NO_2) does not precede the reduction, that is the species being reduced is HNO_3^-, and not NO_2. This conclusion[96] is confirmed by the fact that, judging from the rapid increase in the LPE signal, the rate of reduction is greater than 10 cm s^{-1} ($\kappa > \sqrt{D/\tau}$), whereas the reduction of NO_2 is a much slower process. The addition of different PD to the solution increases the rate of protonation of NO_3^{2-} (the rate constants are given in Table 6), and suppresses the oxidation wave. The published data[95,96] indicate that the electrochemical reduction of NO_3^- to NO_2^-, which is associated with a high overvoltage and is observed at $-E > 1.6$ V, involves the intermediate formation of the high-energy NO_3^{2-} ion, and, as a result of its rapid oxidation, is a quasi-equilibrium process. The decrease in the overvoltage in the presence of PD, which is also characteristic of various other anions,[101] is due to the increase in the rate of protonation, as a result of which NO_3^{2-} is converted into the HNO_3^- ion being reduced.

The wave for the one-electron reduction of the product of the capture of e_{aq}^- by the NO_2^- ion in neutral solution coincides with the polarographic reduction wave for NO. The characteristic reduction time found by the LPE method is greatest close to the half-wave potential and remains the same ($\sim 4 \times 10^{-7}$ s), independent of the NO_2^- concentration , at more negative potentials.[97] These data show that the species being reduced is NO, and the time for its formation in the decomposition of NO_2^{2-} is 2×10^{-7} s. The reduction of NO is reversible, since it is only if this is the case that the characteristic time, determined by the sum of the rates of the forward and back reactions, can be greatest when these rates are equal. The dependence of $E_{1/2}$ and the form of the wave on the frequency of the periodic photo-emission current Ω corresponds to the reversible reduction (see section IV) only at $\Omega > 10^2$ s^{-1}. At lower frequencies there is observed a component of the current due to subsequent irreversible transformations of NO^- with a characteristic time of $\sim 10^{-2}$ s, which depends on the bulk concentration of NO, proportional to the photo-emission current. These data correspond to the conversion of NO^- into $N_2O_2^-$ by reaction (8), whose rate constant has been measured.[101] In the one-electron reduction of $N_2O_2^-$, as in the bimolecular recombination of NO^-, the hyponitrite ion $N_2O_2^{2-}$ is formed, and its decomposition leads to the appearance of the final reduction product N_2O.

In the presence of PD, the extent of the reduction of NO increases from 1 to 3. The formation of NH_2OH in quantities corresponding to the photo-emission current and $n = 3$ was confirmed by chemical analysis.[98] In addition to the main wave, whose form and position are independent of n, a preliminary wave appears (see Fig. 4), whose height increases with increase in the PD concentration (N_p), reaching 3. Like the main wave, the preliminary wave is reversible. The fact that the values of n are the same for the preliminary wave and the main wave indicates that the reduction of NO to NH_2OH takes place by two parallel channels. The fact that the main wave is independent of N_p indicates that the process taking place by one of the channels, as in the one-electron reduction, includes the formation of NO^- and its protonation (the formation of NOH) and subsequent two-electron reduction. Since the preliminary wave lies in the range of E in which NO is reduced, the existence of the second channel is due to the formation of a new electrochemically active species in the reaction of NO with the PD. According to published suggestions,[102] this species is NOH^+. The height of the preliminary wave increases with decrease in Ω (see Fig. 4), so that the rate of protonation is of the order of Ω and the protonation is the limiting stage of the reduction. The $j(E, \Omega)$ relationship in the preliminary wave is described by the expression

$$j = \left| 1 + \frac{3}{1 + \sqrt{k_5 \Omega / 2 k_4^2}\,(1 + e^{-\eta}\sqrt{k_5/k_{10}})\,\sqrt{2i}} \right|. \quad (67)$$

Here, $\eta = \ln(\kappa_6/\kappa_5) = e/kT(E^0 - E)$, where E^0 is the standard NOH/NOH^+ potential, and the significance of the constants in Eqn. (67) can be seen from Fig. 15. Comparison of Eqn. (67) with the experimental data makes it possible to determine the ratio k_4^2/k_5, which was found to be equal to 10^2 s^{-1}. The $j(E)$ relationship, which corresponds to an effective transfer coefficient of 1, indicates that the reduction of NOH^+ is reversible. It follows from the kinetic LPE curves that the characteristic time of the two-electron reduction of NOH is $\sim 2 \times 10^{-6}$ s. The existence of an equilibrium between NO and NOH^+ means that $k_5 \gg k_{10}$ and the decomposition time of NOH^+ does not exceed 10^{-6}s, while $k_4 > 10^4$ mol^{-1} s^{-1}. The decrease in the height of the preliminary wave with increase in the NO_2^- concentration (N_a) indicates that NO^- and NOH react with NO_2^- according to Eqn. (9). The hyponitrate ion $N_2O_3^{2-}$ formed subsequently decomposes to give N_2O,[103] decreasing the extent of the reduction. The dependence of the limiting low-frequency current of the main wave on N_p and N_a, with allowance for the competition of the protonation of NO^- and reaction (9), has the form

$$j_n = 2\,(1 + (1 + k_7 k_9 N_a / k_8^2 N_p^2)^{-1}), \quad (68)$$

that is j_m depends on N_p^2/N_a, and $k_7 k_9 / k_8^2 \simeq 80$ mol. The nitroxyl radical H_2NO undergoes one-electron reduction at $-E > 0.2$ V (characteristic time less than 10^{-6} s).

Thus at high PD concentrations, NO is reduced quantitatively to hydroxylamine if the concentrations of NO_2^- and NO are so low that reactions (8), (9), and (11) which compete with the protonation do not interfere with the formation of NOH and the reduction of H_2NO. The scheme of transformations of the IS given in Fig. 15 provides a basis for the quantitative description of the concentration dependence, obtained from electrochemical measurements,[104] of the relative yield of the main products of the reduction of N_2O and NH_2OH. It follows from the scheme that only the protonated forms of the IS can be reduced, and that protonation precedes the electrode reaction. The protonation is apparently accompanied by the isomerisation of the IS. Since an O–H bond is formed in NOH^+, the reduction product is NOH. This species should be converted into the more stable form HNO,[105] and its subsequent reduction should also be associated with the formation of an O–H bond, and not N–H. The resulting IS HNOH (zerovalent nitrogen) undergoes isomerisation to H_2NO. It is this more stable radical that is observed in the gas phase[106] and in solution,[107] although in the oxidation of NH_2OH by the OH radical, HNOH is formed initially.[108] The suggestion that the IS undergoes isomerisation is consistent with the observed high rates of the electrode reactions (Table 7), since they are associated with the formation of O–H bonds, as in the rapid reduction of the radicals HCO_2 and HCO (see section VII).

The magnitude of the energy of rupture of the O–H bond in NH_2OH [106] shows that the standard H_2NO/NOH potential is greater than the NO^-/NO potential and that the quantitative transformation of NO into NH_2OH is determined by the latter; the reduction of HNO and H_2NO at $E < E^0$ for the NO^-/NO couple is isothermal. The quantitative transformation of NO into NH_2OH requires the expenditure of free energy (more than 234 kJ mol^{-1}). The standard NOH/NO potential, corresponding to $pK(NOH) = 4.7$,[101] is -0.54 V, so that the energy required for the reduction of NO to

NH_2OH in a standard solution with pH = 0 is greater than 155 kJ mol^{-1}, despite the fact that the process as a whole is exothermic (the standard NH_2OH/NO potential is +0.38 V).

The values of the ψ_1-potential appearing in Eqns. (65) and (66) coincide with the total decrease in the potential in the diffuse layer ψ_{10} only for dilute solutions ($\leqslant 10^{-2}$ M), where $x_0 \geqslant 2$ nm.[95] In more concentrated solutions, $|\psi_1| < |\psi_{10}|$. The difference between ψ_1 and ψ_{10} indicates that the NO_3^{2-} anion is discharged at a distance of 0.5–0.7 nm from the plane of maximum approach. The distance of electron transfer, which is several times greater than the geometric dimensions of the ion, is typical of tunnel reactions.[109] The probability of tunnel electron transfer from the reaction complex to the metal, W_0, is related to the rate constant of the oxidation by the simple expression $\kappa = W_0/a$, where a characterises the decrease in the electron density with increase in the distance. The values found[95] for κ correspond, in particular, to electron transfer through a parabolic barrier with a height of ~2 eV. As in ELH reactions (see section VI), the $\kappa(E)$ relationship is determined by the change in the height of the barrier with change in the potential.

The energy of reorganisation of the medium in the reduction of NO to NO^-, not associated with intramolecular rearrangement, can be estimated from the value of κ at $E = E^0$ using Marcus' equation[47] with a reasonable value of the pre-exponential term ($\leqslant 10^{14}$ s^{-1}). According to Benderskii and co-workers,[97] $E_s \simeq 135$ kJ mol^{-1}, which agrees with estimates of E_s in ELH reactions and in the reduction of organic radicals (section IX).

XI. Reduction of ions with anomalous valence

The homogeneous reactions of cations with anomalous valence have been studied in detail under pulse radiolysis conditions. Since the rate constants for the reduction of NO_3^-, NO_2^-, and hydroxyalkyl radicals by Zn^+, Ni^+, and Cd^+ ions are close to the diffusion values,[110] these reactions are exothermic, and the redox potentials for the formation of these ions from the divalent ions should be smaller than −1.5 V. According to published estimates,[111,112] $-E^0$ for the Ni^+/Ni^{2+} couple is greater than 1.8 V, and that for the Pb^+/Pb^{2+}- couple lies in the range 1.1–1.5 V. Comparison of E^0 with the half-wave potentials $E_{1/2}$ for the reduction of the corresponding divalent ions to the metal shows that the intermediate formation of the monovalent cations in this two-electron process is unlikely. According to LPE data the oxidation of the Cd^+, Zn^+, and Ni^+ ions on mercury in the range $E > E_{1/2}$ takes place in less than 10^{-7} s.

The many-electron reduction of anions has been studied by LPE for NO_3^-, NO_2^- (see section X) and BrO_3^-.[113–115] The product of the capture e_{aq}^- by the bromate ion is the BrO_2 radical, whose time-resolved polarograms (see Fig. 6) correspond to its five-electron reduction to Br^- with $E_{1/2} = -1.0$ V. An unexpected result is the value $j = 3$ in the range $E > E_{1/2}$, which formally corresponds to the one-electron reduction of the bromite ion BrO_2^-, although its half-wave potential is −0.88 V,[116] whereas $j = 3$ as far as $E = -0.3$ V, where the BrO_2^- ion is known to be electrochemically stable. The disproportionation of BrO_2^- to give BrO_3^- and BrO^- is also too slow to explain its reduction in 10^{-4} s. The observed increase in j is due to the ion–radical reaction

$$BrO_2 + BrO_2^- \rightarrow BrO + BrO_3^-, \qquad (69)$$

analogous to the transfer of O^- between the reagents, whose rate constants for exothermic reactions are close to the diffusion values.[117] Reaction (69) gives the BrO radical, which is reduced to Br^-, since the product of its one-electron reduction, that is the BrO^- anion, is electrochemically active at $E \leqslant 0$.[116] In reaction (69) with the subsequent three-electron reduction of BrO, only half of the BrO_2 radicals are converted into Br^-, that is $j = 3$. The scheme for the reduction of BrO_3^- at $E > E_{1/2}$ has the form:

$$BrO_3^- \xrightarrow{e^-} BrO_2 \xrightarrow{e^-} BrO_2^- \quad BrO \xrightarrow{e^-} BrO^- \xrightarrow{2e^-} Br^-. \qquad (70)$$

The kinetic LPE curves divide into sections, well separated in time, corresponding to the successive reduction of BrO_2 to BrO_2^- ($n = 1$, the characteristic time decreases from 3×10^{-6} s to 5×10^{-7} s in the range of E values from −0.70 V to −0.95 V) and of BrO^- to Br^- ($n = 2$, τ decreases from 4×10^{-3} s to 6×10^{-5} s in the range of E values from −0.4 V to −0.9 V). For $E < E_{1/2}$, the rate of the reduction of BrO_2^- is greater than the rate of reaction (69), so that $j = 6$. The kinetic LPE curves are described by the relationship

$$Q/Q_m = 6 - 4w(\varkappa_2 \sqrt{t/D}), \qquad (71)$$

where κ_2 is the rate constant of the reduction of BrO_2^- to BrO, which is the limiting stage of the overall process.

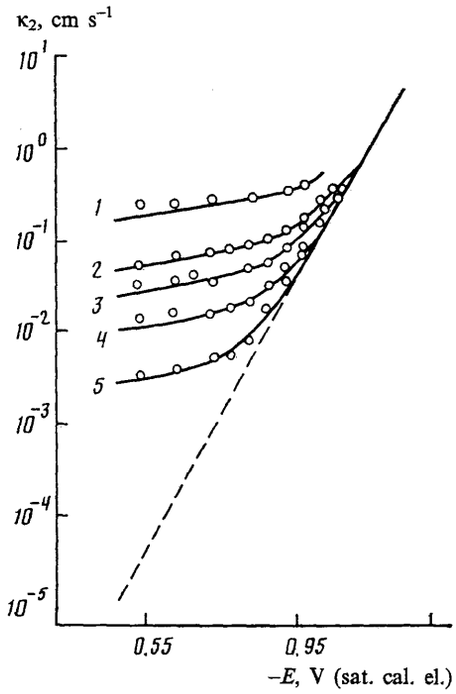


Figure 16. Dependence of the rate constant of the reduction of the BrO_2 radical on the electrode potential at NH_4^+ concentrations, M: *1*, 3.8×10^{-2}; *2*, 1.1×10^{-2}; *3*, 6×10^{-3}; *4*, 3×10^{-3}; and *5*, 1.5×10^{-3}; the broken straight lines corresponds to $N_p = 0$.[115]

Adding NH_4^+ ions to the solution leads to qualitative changes in the polarograms and the kinetic LPE curves. Increase in N_p is accompanied by an increase in $E_{1/2}$ and j for $E > E_{1/2}$ (for

$N_p > 7 \times 10^{-2}$ M, $j = 6$ throughout the working range of E), and the characteristic reduction time decreases rapidly. These changes are due to the increase in κ_2 as a result of the participation of PD in the electrode reaction

$$BrO_2^- + e^- + NH_4^+ \rightarrow BrO + OH^- + NH_3. \quad (72)$$

The $\kappa_2(E)$ relationships for different N_p are given in Fig. 16, and confirm the published conclusion[100,118] that PD take direct part in the reduction of the anions. The rate constant of reaction (72) depends little on E and is close to the diffusion value (~ 5 cm s^{-1}).

XII. Summary

The examination of the electrochemistry of IS opens up new possibilities in the study of both complex many-electron transformations at an interface and the elementary stage of electrode reactions. The significant role of intramolecular reorganisation on electron transfer means that Marcus' model, which takes account of only the reorganisation of the polar medium and for this reason claims to be universal, should be supplemented by an examination of the rearrangement of the reaction complex itself and its solvate layer. In the present state of quantum chemistry, these calculations are becoming possible. Allowance for these last processes may lead to fundamental changes in existing ideas, since reorganisation of this kind (like reorganisation of the medium) not only creates a dynamic barrier to transfer but also leads to the production of a nuclear configuration favourable for reaction. This last feature, in particular, is the factor responsible for rapid low-temperature solid-phase transformations,[119] and possibly plays an equally important role in electrode reactions. The formation of high-energy IS (derivatives of carbene, carbanions, biradicals, etc.), detected by PECR and LPE methods in many electrode reactions, also requires further experimental and theoretical study. The development of these new methods should lead in turn to the development of more selective polarographic analysis, compared with the polarography of stable species.

References

1. A M Bond *Modern Polarographic Methods in Analytical Chemistry* (Translated into Russian), Izd. Khimiya, Moscow, 1983
2. P Toffel, A Henglein *Discuss Faraday Soc.*, 1978, **63** 124
3. A Henglein *Adv. Electroanal. Chem.*, 1976, **9** 163
4. A M Brodskii, Yu Ya Gurevich, Yu V Pleskov, Z A Rotenberg *Sovremennaya Fotoelektrokhimiya. Fotoemissionnye Yavleniya* (Modern Photoelectrochemistry. Photo-emission Phenomena), Izd. Nauka, Moscow, 1974, 167 pp
5. V A Benderskii, A M Brodskii *Fotoemissiya iz Metallov v Rastvory Elektrolitov* (Photo-emission from Metals into Solutions of Electrolytes), Izd. Nauka, Moscow, 1977, 303 pp
6. G C Barker *Ber. Bunsenges. Phys. Chem.*, 1971, **75** 728
7. L I Korshunov, Ya M Zolotovitskii, V A Benderskii *Usp. Khim.*, 1971, **40**(8) 1511 [English translationin *Russ. Chem. Rev.*, 1971(8)]
8. G C Barker, D McKeown, M J Williams, et al. *Discuss. Faraday Soc.*, 1974, **56** 41
9. S D Babenko, V A Benderskii, Ya M Zolotovitskii, A G Krivenko *J. Electroanal. Chem. Interfacial Electrochem.*, 1977, **76** 347
10. M Anbar *Selected Specific Rates of Reactions of Transients from Water in Aqueous Solutions. I. Hydrated Electron*, NSRDS–NBS 43, 1973; NSRDS–NBS 43 Suppl., 1975. *III. Hydroxyl Radical*, NSRDS–NBS 59, 1977, Univ. Notre Dame.
11. A K Pikaev, S A Kabakchi *Reaktsionnaya Sposobost' Pervichnykh Produktov Radioliza Vody: Spravochnik* (The Reactivity of the Primary Products of the Radiolysis of Water, A Reference Book), Energoizdat, Moscow, 1982, 201 pp
12. V A Benderskii *J. Electroanal. Chem. Interfacial Electrochem.*, 1977, **76** 327
13. V A Benderskii, A G Krivenko *Elektrokhimiya*, 1986, **22** 735
14. V A Benderskii, G I Velichko, A G Krivenko, A V Yatsenko *VI Vsesoyuznaya Konferentsiya po Elektrokhimii: Tezisy Dokladov* (Summaries of Papers Presented at the Sixth All-Union Conference on Electrochemistry), Vol. 3, Izd. VINITI, Moscow, 1982, p. 264
15. V V Konovalov, A M Raitsimring, Yu D Tsvetkov, V A Benderskii *Chem. Phys.*, 1985, **93** 163
16. V A Benderskii, A G Krivenko, V A Kurmaz, G V Simbirtseva *Elektrokhimiya*, 1986, **22** 915
17. Z A Rotenberg *Elektrokhimiya*, 1984, **20** 1830
18. B B Damaskin, O A Petrii *Vvedenie v Elektrokhimicheskuyu Kinetiku* (Introduction to Electrochemical Kinetics), Izd. Vys. Shkola, 1983, 400 pp
19. Z A Rotenberg, Yu Ya Gurevich *J. Electroanal. Chem. Interfacial Electrochem.*, 1975, **66**, 165
20. Z A Rotenberg, Ya Kh Threfts *Elektrokhimiya*, 1983, **19** 1129
21. Z A Rotenberg, N M Rufman *Elektrokhimiya*, 1983, **19** 1349
22. V A Benderskii, A G Krivenko, E A Ponomarev *Elektrokhimiya*, 1989, **25** 186
23. V A Benderskii, A G Krivenko, E A Ponomarev *Elektrokhimiya*, 1990 (in the press)
24. V A Benderskii A G Krivenko, V A Kurmaz, G V Simbirtseva *Elektrokhimiya*, 1986, **22** 915
25. V A Benderskii, A G Krivenko *Elektrokhimiya*, 1985, **21** 1507
26. M Graetzel, A Henglein, J Lilie, M Scheffler *Ber. Bunsenges. Phys. Chem.*, 1972, **76** 67
27. A N Frumkin, V A Bagotskii, Z A Iofa *Kinetika Elektrodnykh Protsessov* (The Kinetics of Electrode Processes), Izd. Moskov. Gos. Univ., Moscow, 1952, Chapter 3
28. L I Krishtalik *Elektrodnye Reaktsii. Mekhanizm Elementarnogo Akta* (Electrode Reactions. The Mechanism of the Elementary Act), Izd. Nauka, Moscow, 1979, 223 pp
29. V A Benderskii, A A Ovchinnikov *Fizicheskaya Khimiya. Sovremennye Problemy* (Present-day Problems in Physical Chemistry), Vol. 1, Izd. Khimiya, Moscow, 1980, p. 202
30. Yu V Pleskov, Z A Rotenberg, V V Eletskii *Discuss. Faraday Soc.*, 1974, **56** 52
31. S D Babenko, V A Benderskii, A G Krivenko *J. Electroanal. Chem. Interfacial Electrochem.*, 1977, **84** 33
32. R Parsons, G Picq, P Vennerea *J. Electroanal. Chem. Interfacial Electrochem.*, 1983, **146** 123
33. G A Presland, D R Whitehouse *J. Electroanal. Chem. Interfacial Electrochem.*, 1986, **208** 219
34. S D Babenko, V A Benderskii, A G Krivenko, A A Ovchinnikov *Dokl. Akad. Nauk SSSR*, 1977, **235** 835

35. A A Ovchinnikov, V A Benderskii, S D Babenko, A G Krivenko *J. Electroanal. Chem. Interfacial Electrochem.*, 1978, **91** 321
36. A G Krivenko, A B Vekin, V A Benderskii *Elektrokhimiya*, 1987, **23** 755
37. L I Krishtalik *Adv. Electrochem. Electrochem. Eng.*, 1970, 7 283
38. V A Benderskii, G I Velichko *Usp. Khim.*, 1988, **57**(7) 1065 [English Translation in *Russ. Chem. Rev.*, 1988(7)]
39. V A Benderskii, A G Krivenko, A A Ovchinnikov *J. Electroanal. Chem. Interfacial Electrochem.*, 1980, **111** 19
40. S D Babenko, V A Benderskii, A G Krivenko, S V Sorokin *J. Electroanal. Chem. Interfacial Electrochem.*, 1980, **140** 23
41. H W Nuernberg *Fortsch. Chem. Fortsch.*, 1967, **8** 242
42. L I Krishtalik *Usp. Khim.*, 1965, **34**(11) 1931 [English translation in *Russ. Chem. Rev.*, 1965(11)]
43. A N Frumkin *Adv. Electrochem. Electrochem. Eng.*, 1961, **1** 65; 1963, **3** 287
44. V A Benderskii, A A Ovchinnikov *Dokl. Akad. Nauk SSSR*, 1978, **243** 393
45. A A Ovchinnikov, V A Benderskii *J. Electroanal. Chem. Interfacial Electrochem.*, 1979, **100** 563
46. V A Benderskii, Yu I Dakhnovskii, A A Ovchinnikov *J. Electroanal. Chem. Interfacial Electrochem.*, 1983, **148** 161
47. R A Marcus *Annu. Rev. Phys. Chem.*, 1964, **15** 155
48. R R Dogodnadze, A M Kuznetsov *Itogi Nauki i Tekhniki. Elektrokhimiya* (Progress in Science and Technology. Electrochemistry), Izd. VINITI, Moscow, 1969, p. 5
49. P G Russell, N Kovac, S Srinivasan, M Steinberg *J. Electrochem. Soc.*, 1977, **124** 1329
50. K D Asmus, A Henglein, A Wigger, G Beck *Ber. Bunsenges. Phys. Chem.*, 1966, **70** 756
51. A Henglein *Ber. Bunsenges. Phys. Chem.*, 1974, **78** 1078
52. M Graetzel *Ber. Bunsenges. Phys. Chem.*, 1976, **80** 547
53. D J Schiffrin *Discuss. Faraday Soc.*, 1974, **56** 75
54. V A Benderskii, A G Krivenko *Dokl. Akad. Nauk SSSR*, 1986, **291** 1395
55. W J Albery *Annu. Rev. Phys. Chem.*, 1980, **31** 227
56. S D Babenko, V A Benderskii, A G Krivenko, V A Kurmaz *J. Electroanal. Chem. Interfacial Electrochem.*, 1983, **159** 163
57. S D Babenko, V A Benderskii, A G Krivenko, V A Kurmaz *Elektrokhimiya*, 1983, **19** 1502
58. G V Buxton, R M Sellers *J. Chem. Soc., Faraday Trans. 1*, 1973, **1** 555
59. W Paik, T N Andersen, H Eyring *Electrochim. Acta*, 1969, **14** 1217
60. V A Benderskii, A G Krivenko, V A Kurmaz *Elektrokhimiya*, 1987, **23** 625
61. J D Goddard, H F Schaefer *J. Chem. Phys.*, 1979, **70** 5117
62. R R Lucchese, H F Schaefer *J. Am. Chem. Soc.*, 1978, **100** 298
63. M J H Kemper, J M F Van Dijk, H M Buck *J. Am. Chem. Soc.*, 1978, **100** 7841
64. Z A Rotenberg, N M Rufman *Elektrokhimiya*, 1984, **20** 771
65. V A Benderskii, A G Krivenko, V A Kurmaz *Dokl. Akad. Nauk SSSR*, 1984, **278** 898
66. V A Benderskii, A G Krivenko, V A Kurmaz *Elektrokhimiya*, 1986, **22** 644
67. S Clarke, J A Harrison *J. Electroanal. Chem. Interfacial Electrochem.*, 1972, **36** 109
68. P Valenta *Collect. Czech. Chem. Commun.*, 1960, **25** 853
69. S Wolfe, L M Tel, I G Csizmadia *Can. J. Chem.*, 1973, **51** 2423
70. V P Glushko (Editor) *Termodinamicheskie Svoistva Individual'nykh Veshchestv: Tablitsy Prinyatykh Znachenii* (The Thermodynamic Properties of Individual Substances: Tables of Accepted Values), Vol. 4, Izd. VINITI, Moscow, 1979, 558 pp
71. A P Tomilov, S G Mairanovskii, M Ya Fioshin, V A Smirnov *Elektrokhimiya Organicheskikh Soedinenii* (The Electrochemistry of Organic Compounds), Izd. Khimiya, Moscow, 1968, Chapter 6
72. N S Hush, K B Oldham *J. Electroanal. Chem. Interfacial Electrochem.*, 1963, **6** 34
73. R C Heaton, H A Laitinen *Anal. Chem.*, 1974, **46** 547
74. K P Butin, V V Strelets, A N Kashin, et al. *J. Organomet. Chem.*, 1974, **64** 181
75. M Graetzel, K M Bansal, A Henglein *Ber. Bunsenges. Phys. Chem.*, 1973, **77** 11
76. V A Benderskii, A G Krivenko, V A Kurmaz *Elektrokhimiya*, 1986, **22** 644
77. O R Brown, K Lister *Discuss. Faraday Soc.*, 1968, **45** 106
78. H Kita, A Katayama *Electrochim. Acta*, 1974, **19** 555
79. E Muller *Z. Elektrochem.*, 1927, **23** 253
80. S G Mairanovskii *Catalytic and Kinetic Waves*, Plenum Press, New York, 1968, Chapter 3
81. P J Elving *Can. J. Chem.*, 1977, **55** 3392
82. V A Benderskii, A G Krivenko, G V Simbirtseva *Elektrokhimiya*, 1987, **23** 748
83. G B Ellison, P C Engelking, W C Lineberger *J. Am. Chem. Soc.*, 1978, **100** 2557
84. S Wolfe, L M Tel, I G Csizmadia *Can. J. Chem.*, 1973, **51** 2423
85. C A Banton *Nucleophilic Substitution at Saturated Carbon Atom*, Elsevier Publ., New York, 1963, Chapters 2, 3
86. D J Cram *Organic Chemistry, Vol. 4, Fundamentals of Carbanion Chemistry* (Translated into Russian), Izd. Mir, Moscow, 1967, 300 pp
87. A Streitwieser, J H Hammons *Prog. Phys. Org. Chem.*, 1965, **3** 1
88. O A Reutov, I P Beletskaya, K P Butin *CH-Kisloty* (CH-Acids), Izd. Nauka, Moscow, 1980, 247 pp
89. J E Bartmess, J A Scott, R T McIver *J. Am. Chem. Soc.*, 1979, **101** 6046
90. K E Edgecombe, R J Russell *Can. J. Chem.*, 1984, **62** 2887
91. M H Abraham, A F Danil de Namor *J. Chem. Soc., Faraday Trans. 1*, 1978, **74** 2102
92. J O'M Bockris, S U M Khan *Quantum Electrochemistry*, Plenum Press, New York, 1979, Chapter 6
93. J O'M Bockris, S U M Khan *J. Phys. Chem.*, 1983, **87** 2599
94. A A Ovchinnikov, M Ya Ovchinnikova *Zh. Eksp. Teor. Fiz.*, 1969, **56** 1278
95. E A Ponomarev, A G Krivenko, V A Benderskii, N V Fedorovich *Elektrokhimiya*, 1987, **23** 867
96. E A Ponomarev, A G Krivenko, V A Benderskii, N V Fedorovich *Elektrokhimiya*, 1987, **23** 1441
97. V A Benderskii, A G Krivenko, E A Ponomarev *Elektrokhimiya*, 1989, **25** 178
98. V A Benderskii, A G Krivenko, E A Ponomarev *Dokl. Akad. Nauk SSSR*, 1989 (in the press)
99. M Graetzel, S Taniguchi, A Henglein *Ber. Bunsenges. Phys. Chem.*, 1970, **74** 1003
100. M Graetzel, A Henglein, S Taniguchi *Ber. Bunsenges. Phys. Chem.*, 1970, **74** 292

101. N V Fedorovich *Itogi Nauki i Tekniki. Elektrokhimiya* (Progress in Science and Technology. Electrochemistry), Vol. 14, Izd. VINITI, Moscow, 1978, p. 5
102. D L Ehman, D T Sawyer *J. Electroanal. Chem. Interfacial Electrochem.*, 1968, **16** 541
103. C C Addison, G A Gamlen, P Thompson *J. Chem. Soc.*, 1952, 338
104. R K Kvaratskheliya *Elektrokhimicheskoe Vosstanovlenie Kislorodsoderzhashchikh Soedinenii Azota* (The Electrochemical Reduction of Oxygen-Containing Compounds of Nitrogen), Izd. Metsniereba, Tbilisi, 1987, 106 pp
105. S Saito, K Takagi *J. Mol. Spectrosc.*, 1973, **47** 99
106. P B Davies, P Dransfeld, F Temps, H G Wagner *J. Chem. Phys.*, 1984, **81** 3763
107. S P Mishra, M C R Symons *J. Chem. Res.*, 1977, 2078
108. M Simic, E Hayon *J. Am. Chem. Soc.*, 1971, **93** 5982
109. K I Zamaraev, R F Khairutdinov, V P Zhdanov *Tunnelirovanie Elektrona v Khimii* (Electron Tunnelling in Chemistry), Izd.Nauka, Novosibirsk, 1985, 317 pp
110. G V Buxton, R M Sellers *Compilation of Rate Constants for the Reactions of Metal Ions in Unusual Valency States*, NSRDS–NBS 62, 1978
111. M Kelm, J Lilie, A Henglein, E Janata *J. Phys. Chem.*, 1974, **78** 882
112. J H Baxendale *Z. Phys. Chem.*, 1964, **43** 161
113. V Concialini, O Tubertini *J. Electroanal. Chem. Interfacial Electrochem.*, 1978, **88** 57
114. V A Benderskii, A G Krivenko, N V Fedorovich *Elektrokhimiya*, 1986, **22** 728
115. V A Benderskii, A G Krivenko, N F Fedorovich *J. Electroanal. Chem. Interfacial Electrochem.*, 1988, **241** 247
116. A F Krivis, G R Supp *Analyt. Chem.*, 1968, **40** 2063
117. A Henglein *Radiat. Phys. Chem.*, 1980, **15** 151
118. B B Damaskin, N V Fedorovich, F S Sarbash *J. Electroanal. Chem. Interfacial Electrochem.*, 1982, **135** 181
119. V I Goldanskii, V A Benderskii, L I Trachtenberg *Adv. Chem. Phys.*, 1989, **73** 349